DOI: 10.1002/chem.200701636

Modular Phosphite–Oxazoline/Oxazine Ligand Library for Asymmetric Pd-Catalyzed Allylic Substitution Reactions: Scope and Limitations—Origin of Enantioselectivity

Montserrat Diéguez* and Oscar Pàmies*[a]

Dedicated to Professor Jan-E. Bäckvall on his 60th birthday

Abstract: A library of phosphite–oxazoline/oxazine ligands **L1**–**L15a**–**h** has been synthesized and screened in the Pd-catalyzed allylic substitution reactions of several substrate types. These series of ligands can be prepared efficiently from easily accessible hydroxyl amino acid derivatives. Their modular nature enables the substituents/configurations in the oxazoline/oxazine moiety, alkyl backbone chain and in the biaryl phosphite moiety to be easily and systematically varied. By carefully selecting the ligand components, therefore, high regio- and enantioselectivities (*ee* values up to 99%) and good activities have been achieved in a broad range of mono- and disubstituted linear hindered and unhindered liner and cyclic substrates. The NMR studies on the Pd–π-allyl intermediates provide a deeper understanding about the effect of the ligand parameters on the origin of enantioselectivity. It also indicates that the nucleophilic attack takes place predominantly at the allylic terminal carbon atom located *trans* to the phosphite moiety.

Keywords: asymmetric catalysis · chiral ligands · palladium · reaction mechanisms

Introduction

Palladium-catalyzed asymmetric allylation of nucleophiles is recognized to be useful for organic synthesis, allowing the formation of enantioselective carbon–carbon and carbon–heteroatom bonds.[1] Many chiral ligands (mainly P and N ligands), which possess either C_2 or C_1 symmetry, have provided high enantiomeric excesses for several types of disubstituted substrates.[1] Although, in general, there is still a problem of substrate specificity (for example, *ee* values are high in disubstituted linear hindered substrates and low in unhindered substrates, and vice versa) and reaction rates. On the other hand, monosubstituted substrates still require more active and more regio- and enantioselective Pd catalysts.[1] Most chiral ligands developed for Pd-catalyzed asymmetric allylic substitution are mixed bidentate donor ligands (such as P-N, P-S, S-N and P-P′).[1–3] The efficiency of this type of hard–soft heterodonor ligands has mainly been attributed to the electronic effects of the donor atoms. Mixed phosphorus–nitrogen ligands have played a dominant role among heterodonor ligands. One of the most important series of ligands developed for this process is the phosphine–oxazoline PHOX ligands **1** (Figure 1).[4] We have recently demonstrated that replacing the phosphine moiety in the PHOX ligand family (Figure 1, ligands **1**) with a biaryl phosphite (Figure 1, ligands **2**) is highly advantageous since it overcomes the most common limitations of this process, such as low reaction rates and high substrate specificity.[5] These phosphite–oxazoline ligands **2** have therefore provided excellent enantioselectivities and activities in several substrate types.[5] Using biaryl phosphites was beneficial because: 1) reaction rates increased thanks to the larger π-acceptor ability of the phosphite moiety,[5,6] 2) substrate specificity decreased because the chiral pocket created (the chiral cavity in which the allyl is embedded) is flexible enough to enable perfect coordination of hindered and unhindered substrates,[7] and 3) regioselectivity towards the desired branched isomer in monosubstituted linear substrates increased thanks to the π-acceptor ability of the phosphite moiety that enhances the S_N1 character of the nucleophilic attack.[8]

[a] Dr. M. Diéguez, Dr. O. Pàmies
Departament de Química Física i Inorgànica
Universitat Rovira i Virgili. Campus Sescelades
C/Marcel·lí Domingo, s/n. 43007 Tarragona (Spain)
Fax: (+34) 977-559-563
E-mail: montserrat.dieguez@urv.cat
oscar.pamies@urv.cat

Supporting information for this article is available on the WWW under http://www.chemeurj.org/ or from the author.

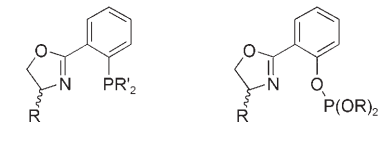

Figure 1. Phosphine–oxazoline (PHOX) and phosphite–oxazoline ligands **1** and **2**.

Despite such success, little attention has been paid to this new class of highly efficient ligands for this process[7b,8,9] and a systematic study of the potential of phosphite–oxazoline as new ligands is still needed. Therefore, more research needs to be done to understand the role of several ligand parameters in the origin of stereochemistry of the allylic substitution reactions. In this context, the mechanistic aspects with these ligands are still not understood well enough for a priory prediction of the type of ligand needed for high selectivity. For this purpose, in this paper we extend our 2005 study of phosphite–oxazoline ligands **2**[5] (Figure 1) to other phosphite–oxazoline/oxazine ligands **L1**–**L15a**–**h** in which the oxazoline/oxazine and phosphite donor moieties are connected by a chiral alkyl backbone chain (Figure 2).

Interestingly, one of the advantage of this new ligand library design is that more ligand parameters, which are important for the allylic substitution reactions, can be easily introduced, and therefore studied, than in our first generation of phosphite–oxazoline ligands **2** (Scheme 1). In the first generation, for example, the oxazoline substituent was restricted to those found in readily available amino alcohols. In the second generation, these substituents are introduced from carboxylic acid derivatives, which enables the introduction of almost any substituent.

Here we therefore report the synthesis and application of a new chiral phosphite–oxazoline and phosphite–oxazine ligand library (**L1**–**L15a**–**h**, Figure 2) for the Pd-catalyzed allylic substitution reactions of several substrates types. We also discuss the synthesis and characterization of the Pd–π-allyl intermediates in order to provide greater insight into the origin of enantioselectivity with these catalytic systems. The library was synthesized and screened using a series of parallel reactors each equipped with 12 different positions. As well as a biaryl phosphite moiety being present in the

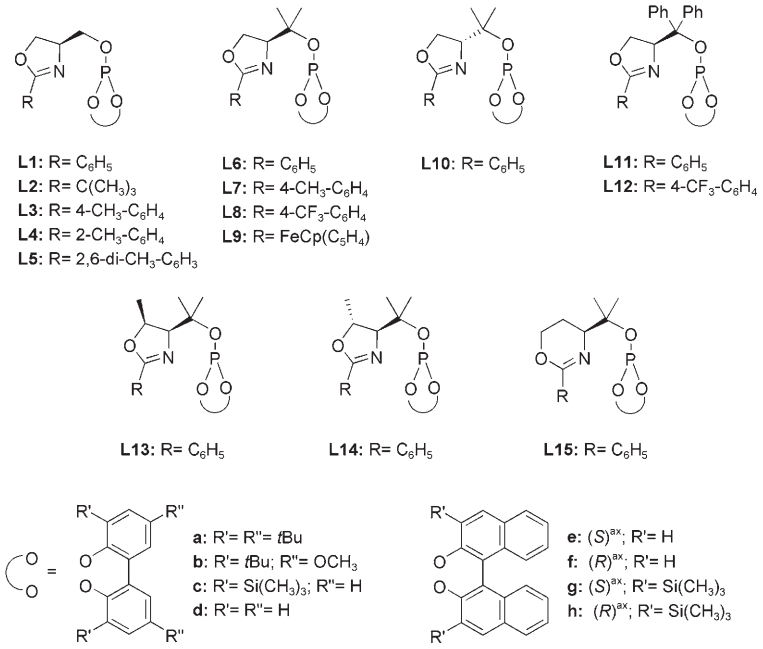

Figure 2. New phosphite–oxazoline and phosphite–oxazine ligand library **L1**–**L15a**–**h**.

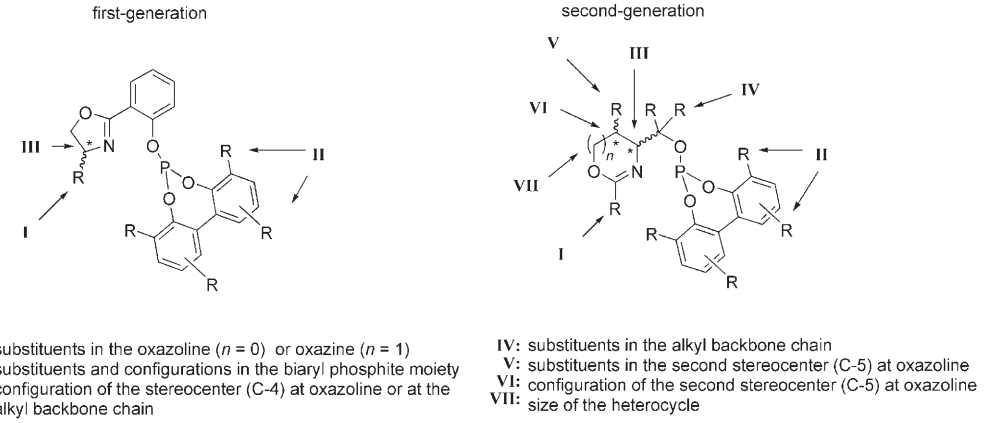

Scheme 1. Basic framework of our first and second generations of phosphite–oxazoline/oxazine ligand libraries showing the ligand parameters that can be studied.

ligand design, this ligand library also has the advantage of a flexible ligand scaffold that enables the ligands to be easily tuned in different ligand parameters and how the ligands affect catalytic performance to be explored. With this library (Figure 2), we therefore investigated the effect of systematically varying the substituents in the oxazoline/oxazine (R) moiety and in the alkyl backbone chain (H, **L1**–**L5**, Me, **L6**–**L9** and Ph, **L11**–**L12**). We also studied the configuration of the alkyl backbone chain (ligands **L6** and **L10**), the presence of a second stereogenic center in the heterocycle ring and its configuration (ligands **L13** and **L14**), the size of the heterocycle (ligand **L15**) and the substituents and configurations in the biaryl phosphite moiety (**a**–**h**). By carefully selecting the ligand parameters, we achieved high selectivities (regio- and enantioselectivities) and activities in different substrate types.

Results and Discussions

Synthesis of ligand libraries: The sequence of ligand synthesis is illustrated in Scheme 2. Ligand synthesis is straightforward (Scheme 2). The ligands were synthesized very efficiently from the corresponding easily accessible hydroxyl amino acid derivatives (**3**–**7**, Scheme 2). Compounds **3**–**6** are commercially available and **7**[10] is easily made in two steps from (*S*)-homoserine. The compounds **3**–**7** were chosen as starting materials for the preparation of ligands **L1**–**L15a**–**h** because they already incorporate the various elements that will enable us to study the configuration of the alkyl backbone chain (**3** and **4**), the presence of a second stereogenic center in the heterocycle as well as its configuration (**5** and **6**) and the heterocycle ring size (**3** and **7**). In the first step of the ligand synthesis (Scheme 2, step a), compounds **3**–**7** were coupled with the corresponding acid chlorides in the presence of triethylamine to produce the desired amides **8**–**14**, **33**, **36**, **39**, **42** (See Experimental Section). They were then converted to the corresponding oxazoline esters **15**–**21**, **34**, **37**, **40** and oxazine ester **43** in the presence of diethylaminosulfur trifluoride (DAST), (Scheme 2, step b, See Experimental Section). Note that the ring closure follows an S_N2-like pathway, so for oxazolines **37** and **40**, the absolute configuration of the stereogenic methyl group is inverted. In the next step the desired diversity in the substituents of the alkyl backbone chain is reached (-H, -Me, -Ph). The reduction of the oxazoline/oxazine esters therefore afforded the corresponding hydroxyl oxazolines/oxazines compounds **22**–**32**, **35**, **38**, **41** and **44** (see Experimental Section). At this point, the choice of reducing agent is crucial to introducing the desired substituents in the alkyl backbone chain (-H, -Me, -Ph). Using $LiAlH_4$, therefore, we obtained compounds **22**–**26** with hydrogen substituents in the alkyl backbone chain (Scheme 2, step c). When we used the Grignard reagents (either CH_3MgCl or PhMgCl) on the other hand, we obtained compounds **27**–**30**, **35**, **38**, **41** and **44** (with methyl substituents, Scheme 2, step d) and compounds **31** and **32** (with phenyl substituents, Scheme 2, step e). In the last step (Scheme 2, step f), treating the corresponding hydroxyl-oxazoline/oxazine with one equivalent of the appropriate in situ formed phosphorochloridite ($ClP(OR)_2$; $(OR)_2$ = **a**–**h**) in the presence of pyridine provided easy access to the desired phosphite–oxazoline/oxazine ligands **L1**–**L15a**–**h**.

All ligands were stable during purification on neutral alumina under an atmosphere of argon and they were isolated as white solids. They were stable at room temperature and very stable to hydrolysis. Elemental analyses were in agreement with the structure assigned. The ^1H and ^{13}C NMR spectra were as expected for these C_1 ligands. One singlet for each compound was observed in the ^{31}P NMR spectrum (see Experimental Section). Rapid ring inversions (atropoisomerization) in the biphenyl-phosphorus moieties (**a**–**d**) occurred on the NMR time scale since the expected diastereoisomers were not detected by low-temperature phosphorus NMR.[11]

Allylic substitution of disubstituted linear substrates: In this section we report the use of the chiral phosphite–oxazoline (**L1**–**L14a**–**h**) and phosphite–oxazine (**L15a**) ligands in the Pd-catalyzed allylic substitution [Eq. (1)] of three linear substrates with different steric properties: *rac*-1,3-diphenyl-3-acetoxyprop-1-ene (**S1**) (widely used as a model substrate), *rac*-(*E*)-ethyl 2,5-dimethyl-3-hex-4-enylcarbonate (**S2**) and *rac*-1,3-dimethyl-3-acetoxyprop-1-ene (**S3**). Two nucleophiles were tested. In all cases, the catalysts were generated in situ from π-allyl–palladium chloride dimer $[PdCl(\eta^3\text{-}C_3H_5)]_2$ and the corresponding ligand.[1]

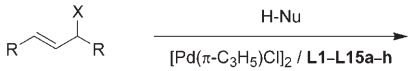

(1)

S1: R= Ph; X= OAc
S2: R= *i*Pr; X= OCO_2Et
S3: R= Me; X= OAc

45: R= Ph; H-Nu= H-CH(COOMe)$_2$
46: R= Ph; H-Nu= H-NHCH$_2$Ph
47: R= *i*Pr; H-Nu= H-CH(COOMe)$_2$
48: R= *i*Pr; H-Nu= H-NHCH$_2$Ph
49: R= Me; H-Nu= H-CH(COOMe)$_2$
50: R= Me; H-Nu= H-NHCH$_2$Ph

Allylic substitution of* rac-*1,3-diphenyl-3-acetoxyprop-1-ene (S1) using dimethyl malonate and benzylamine as nucleophiles [Eq. (1)]: For an initial evaluation of this new type of ligand in the palladium-catalyzed asymmetric substitution reactions, we chose the allylic substitution of **S1** (equation 1, R = Ph; X = OAc) and used dimethyl malonate and benzylamine as nucleophiles. As these reactions were carried out with a variety of ligands carrying different donor groups, we could easily compare the efficacy of the various ligand systems.[1]

In the first set of experiments, we determined the optimal reaction conditions by conducting a series of experiments in which the solvent and ligand-to-palladium ratio were varied. We first studied the effect of four solvents (tetrahydrofuran (THF), toluene, dimethylformamide (DMF) and dichloromethane (DCM)) with five ligands (**L1a**, **L6a**, **L12a**, **L13a**, **L15a**). Figure 3 shows the results when dimethyl malonate

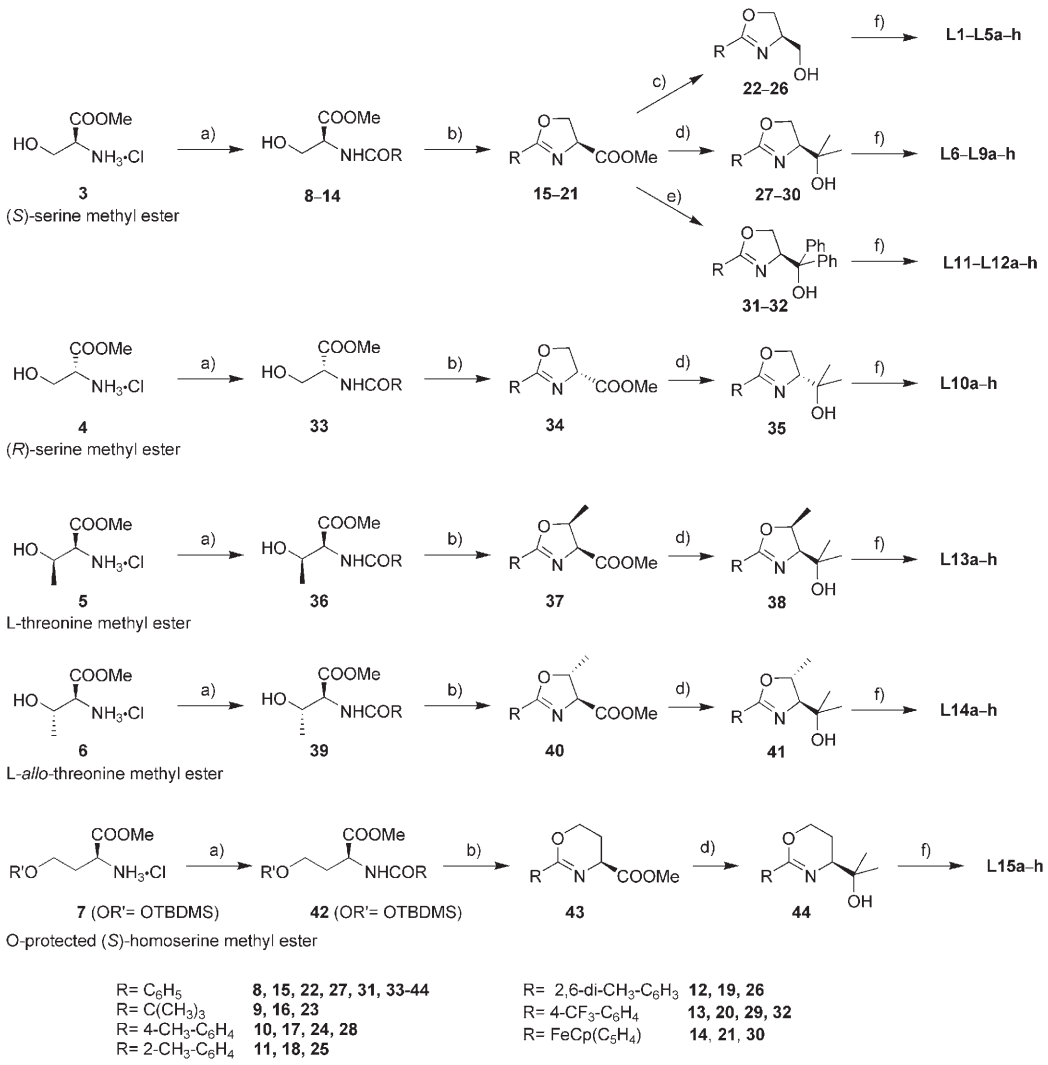

Scheme 2. Synthesis of phosphite–oxazoline and phosphite–oxazine ligand library **L1–L15a–h**. a) $RCOCl/NEt_3/CH_2Cl_2$ (yields 85–99%). b) DAST/CH_2Cl_2 (yields 86–98%). c) $LiAlH_4/Et_2O$ (yields 79–94%). d) CH_3MgCl/Et_2O/THF (yields 81–96%). e) $PhMgCl/Et_2O$/THF (yields 84–93%). f) $ClP(OR)_2$; $(OR)_2$ = **a–h**/Py/toluene (yields 34–81%).

was used as the nucleophile (trends were similar in the allylic amination of **S1**, see Supporting Information). Our results show that the efficiency of the process strongly depended on the nature of the solvent. The best combination of activity and enantioselectivity was achieved with dichloromethane (Figure 3). The enantiomeric excesses (*ee* values) obtained with toluene were comparable to those obtained with dichloromethane, but the activities were lower. Dimethylformamide yielded high relative conversions, similar to those of dichloromethane, but their *ee* values were lower. The lowest *ee* values were obtained when THF was used as solvent. We therefore chose dichloromethane as our solvent.

We then studied the effect of varying the ligand-to-palladium ratio. Conversions and enantioselectivities when dichloromethane was used as a solvent are shown in Table 1 (trends were similar for the other solvents, see Supporting Information). These results show that excess ligand is not necessary. Interestingly using ligand **L2a**, which contains a bulky substituent at the oxazoline moiety, we observed a decrease in the enantioselectivity at a higher ligand-to-palladium ratio of 1. This is due to the fact that at a higher ligand-to-palladium ratio of 1 the phosphite–oxazoline **L2a** ligand acts as a monodentate ligand (see below, Section on Origin of Enantioselectivity).

For the purpose of comparison, the rest of the ligands were tested under conditions that provided optimal enantioselectivities and reaction rates (i.e., a ligand-to-palladium ratio of 1.1 and dichloromethane as solvent). Table 2 shows the results when dimethyl malonate and benzylamine were used as nucleophiles. These results indicate that catalytic performance (activities and enantioselectivities) is affected by the substituents at the oxazoline and at the alkyl backbone chain, the presence of a second stereogenic center in the oxazoline ring, the size of the heterocycle and the substituents/configuration in the biaryl phosphite moiety. Activities >500 mol **S1** $\times$ (mol Pd $\times$ h)$^{-1}$ and enantioselectivities

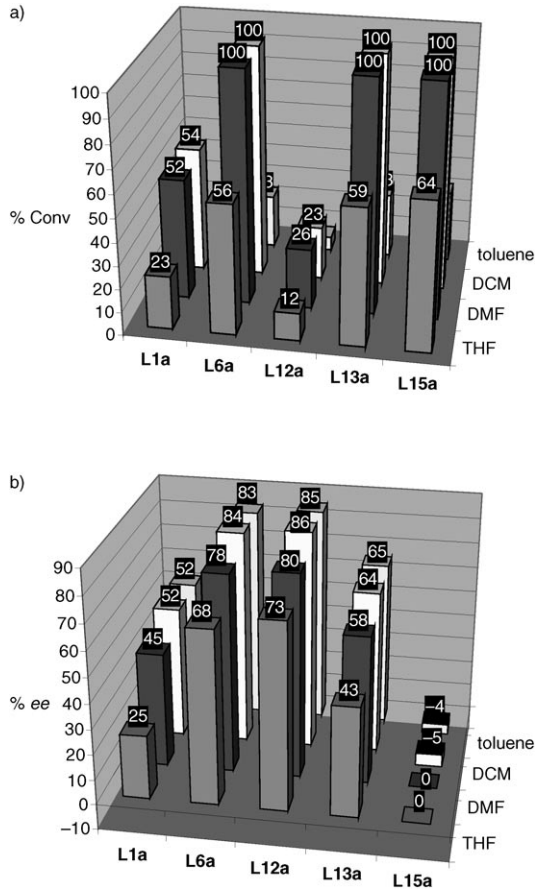

Figure 3. Results of the catalytic allylic alkylation of **S1** using ligands **L1a**, **L6a**, **L12a**, **L13a** and **L15a** in four solvents at room temperature. a) Conversions after 15 minutes. (b) Enantioselectivities of product **45**. Positive numbers refer to the formation of the *S* isomer in excess and negative numbers refer to the formation of *R* isomer.

Table 1. Selected results for the Pd-catalyzed allylic alkylation of **S1** using ligands **L1a**, **L2a**, **L6a** and **L12a**. Effect of the ligand-to-palladium ratio.[a]

Entry	Ligand	L/Pd	Conv [%] (*t* [min])[b]	*ee* [%][c]
1	**L1a**	0.8	95 (30)	47 (*S*)
2	**L1a**	1.1	100 (30)	52 (*S*)
3	**L1a**	2	100 (30)	53 (*S*)
4	**L2a**	0.8	75 (30)	20 (*S*)
5	**L2a**	1.1	85 (30)	14 (*S*)
6	**L2a**	2	100 (15)	5 (*S*)
7	**L6a**	0.8	93 (30)	81 (*S*)
8	**L6a**	1.1	100 (15)	84 (*S*)
9	**L6a**	2	100 (15)	84 (*S*)
10	**L12a**	0.8	84 (60)	85 (*S*)
11	**L12a**	1.1	90 (60)	86 (*S*)
12	**L12a**	2	91 (60)	87 (*S*)

[a] All reactions were run at room temperature. 0.5 mol% $[PdCl(\eta^3\text{-}C_3H_5)]_2$. CH_2Cl_2 as solvent. [b] Conversion percentage determined by ^{1}H NMR. [c] Enantiomeric excesses determined by HPLC on a Chiralcel-OD column. Absolute configuration in parentheses.

up to 96% were obtained. Catalytic performance in the Pd-catalyzed allylic amination of **S1** followed the same trend as for the allylic alkylation of **S1**. As expected, however, activities were lower than in the alkylation reaction. The stereoselectivity of the amination was the same as for the alkylation reaction, though the CIP descriptor was inverted because of the change in the priority of the groups.

The effect of the oxazoline substituent was studied with ligands **L1**–**L9a** (Table 2, entries 1–6, 14–15 and 18). We found that these substituents affected both activities and enantioselectivities. Our results showed that enantioselectivity is dependent on both the electronic and steric properties

Table 2. Selected results for the Pd-catalyzed allylic substitution of **S1** using the P,N ligand library **L1**–**L15a**–**h**.[a]

Entry	Ligand	H-Nu = H-CH(COOMe)$_2$ Conv [%] (*t* [min])[b]	H-Nu = H-CH(COOMe)$_2$ *ee* [%][c]	H-Nu = H-NHCH$_2$Ph Conv [%] (*t* [h])[b]	H-Nu = H-NHCH$_2$Ph *ee* [%][c]
1[d]	**L1a**	100 (30)	52 (*S*)	100 (24)	55 (*R*)
2	**L2a**	85 (30)	14 (*S*)	64 (24)	9 (*R*)
3	**L3a**	100 (30)	46 (*S*)	100 (24)	50 (*R*)
4	**L4a**	94 (30)	30 (*S*)	100 (24)	32 (*R*)
5	**L5a**	84 (30)	3 (*S*)	74 (24)	5 (*R*)
6	**L6a**	100 (15)	84 (*S*)	100 (16)	87 (*R*)
7	**L6b**	100 (15)	85 (*S*)	100 (16)	86 (*R*)
8[d]	**L6c**	100 (15)	89 (*S*)	100 (16)	92 (*R*)
9	**L6d**	98 (30)	90 (*S*)	100 (24)	92 (*R*)
10	**L6e**	99 (30)	90 (*S*)	100 (24)	93 (*R*)
11	**L6f**	84 (30)	89 (*S*)	100 (24)	91 (*R*)
12	**L6g**	100 (25)	55 (*S*)	93 (16)	57 (*R*)
13	**L6h**	100 (25)	88 (*S*)	95 (16)	90 (*R*)
14	**L7a**	100 (15)	82 (*S*)	100 (16)	83 (*R*)
15[d]	**L8a**	100 (15)	90 (*S*)	100 (16)	93 (*R*)
16[d]	**L8c**	100 (15)	92 (*S*)	100 (16)	96 (*R*)
17	**L8e**	64 (30)	83 (*S*)	92 (24)	84 (*R*)
18	**L9a**	36 (15)	78 (*S*)	53 (16)	80 (*R*)
19[d]	**L10a**	100 (15)	85 (*R*)	100 (16)	88 (*S*)
20	**L11a**	90 (60)	86 (*S*)	100 (24)	89 (*R*)
21	**L12a**	88 (60)	86 (*S*)	100 (24)	88 (*R*)
22	**L13a**	100 (15)	64 (*S*)	100 (16)	62 (*R*)
23[d]	**L14a**	100 (15)	82 (*S*)	100 (16)	84 (*R*)
24[d]	**L15a**	100 (15)	5 (*R*)	100 (16)	8 (*S*)

[a] All reactions were run at room temperature. 0.5 mol% $[PdCl(\eta^3\text{-}C_3H_5)]_2$. 1.1 mol% ligand. CH_2Cl_2 as solvent. [b] Conversion percentage determined by ^{1}H NMR. [c] Enantiomeric excesses determined by HPLC. Absolute configuration in parentheses. [d] Isolated yields of **45** and **46** were >93%.

of the substituents in the oxazoline moiety. Bulky substituents in this position therefore decreased enantioselectivities, whereas electron-withdrawing substituents increased *ee* values. Enantioselectivities were best with ligand **L8a**, which contains a 4-CF_3-phenyl-oxazoline group (Table 2, entry 15). However, activities were controlled by the steric properties of the substituents in the oxazoline groups and were higher when less sterically demanding substituents were present (i.e., Ph≈4-R-Ph>2-Me-Ph>*t*Bu≈2,6-diMe-Ph).

We studied the effect of the substituents and the configuration of the alkyl backbone chain using ligands **L1a**, **L6a**, **L10a** and **L11a** (Table 2, entries 1, 6, 19 and 20). With regard to the effect of the substituents of the alkyl chain on catalytic performance, our results show that introducing methyl substituents in this position has an extremely positive effect on activity and enantioselectivity (entries 1 vs 6).

However, while introducing bulkier substituents such as phenyl slightly increased enantioselectivity, activities dropped considerably (entries 6 vs 20). The best trade-off between activity and enantioselectivity was obtained with methyl substituents in the alkyl backbone chain. With regard to the effect of the configuration of the alkyl backbone chain, we found that the sense of enantioselectivity is governed by its absolute configuration (Table 2, entries 6 vs 19). Both enantiomers of the substitution products **45** and **46** can therefore be accessed in good enantioselectivity simply by changing the absolute configuration of the alkyl backbone chain.

The effects of the biaryl phosphite moiety were studied using ligands **L6a–h** (Table 2, entries 6–13). These moieties mainly affected activity and their effect on enantioselectivity was less important. Bulky substituents at the *ortho* positions of the biphenyl moiety therefore increased activity (Table 2, entries 6–8 vs 9–13), while enantioselectivities were slightly better when either disubstituted *ortho* trimethylsilyl (Table 2, entry 8) or unsubstituted biaryl moieties (Table 2, 9–11) were used. The presence of bulky trimethylsilyl substituents in the *ortho* positions of the biphenyl moieties is therefore necessary if both activities and enantioselectivities have to be high. To further investigate how enantioselectivity was influenced by the axial chirality of the biaryl moiety, ligands **L6e–h** containing different enantiomerically pure binapthyl moieties were also tested (Table 2, entries 10–13). For ligands **L6g** and **L6h**, which contain bulky biaryl moieties, our results show a cooperative effect between the configuration of the biaryl phosphite moiety and the configuration of the alkyl backbone chain that resulted in a matched combination for ligand **L6h** (Table 2, entries 12 and 13). Moreover, comparing the results of using ligands **L6c**, **L6g** and **L6h** (Table 2, entries 8 vs 12 and 13) we can conclude that the biphenyl phosphite moiety in ligand **L6c** adopts an *R* configuration upon complexation to the palladium.[12]

To study how a second stereogenic center in the oxazoline and its configuration affect the catalytic performance, we also tested ligands **L13a** and **L14a** (Table 2, entries 22 and 23). The results show a cooperative effect between the configuration of this second stereocenter and the configuration of the alkyl backbone chain on enantioselectivity that results in a matched combination for ligands **L14a**, which contains an *R* configuration at the second stereocenter and an *S* configuration at the alkyl backbone chain (Table 2, entries 22 vs 23).

Finally, we studied the effect of the heterocycle ring size by using ligands **L6a** and **L15a** (Table 2, entries 6 and 24). Our results show that the oxazine moiety is much less enantioselective than its oxazoline counterpart. This can be attributed to the fact that the six-membered cycle of the oxazine moiety is less rigid than the five-membered cycle of the oxazoline unit.

In summary, the best result (on terms of activity and enantioselectivity) was obtained with ligand **L8c** (Table 2, entry 16, TOF's of 500 mol **S1**×(mol Pd×h)$^{-1}$ and *ee* up to 96%), which contains the optimal combination of ligand parameters (substituents at the oxazoline and at the alkyl backbone chain, the size of the heterocycle and the substituents in the biaryl phosphite moiety). Moreover, both enantiomers of substitution products **45** and **46** can be accessed in high enantioselectivity simply by changing the absolute configuration of the alkyl backbone chain. These results clearly show the efficiency of using highly modular scaffolds in the ligand design.

***Allylic substitution of* rac-*(E)*-ethyl-2,5-dimethyl-3-hex-4-enylcarbonate (S2) using dimethyl malonate and benzylamine as nucleophiles [Eq. (1)]**: We screened the phosphite–oxazoline/oxazine ligand library **L1–L15a–h** in the allylic substitution process of **S2** using dimethyl malonate and benzylamine as nucleophiles [Eq. (1), R = *i*Pr, X = OCO_2Et]. This substrate is more sterically demanding than substrate **S1**, which we used before.[1] If *ee* values are to be high, the ligand must create a bigger chiral pocket around the metal center to be able to accommodate the sterically demanding isopropyl substituents.[1] Due to the flexibility conferred by the biaryl phosphite moiety, we expect to obtain also good enantioselectivites for this substrate. The most interesting results are shown in Table 3. In general, the trends were the same as for the allylic substitution of **S1**. Again, the catalyst precursor containing phosphite–oxazoline ligand **L8c** provided the best enantioselectivities (Table 3, entry 11). As expected, the activities were lower than in the alkylation reaction of **S1**.[1] The stereoselectivity of the alkylation of **S2** was the same as for the alkylation reaction of **S1**, though the CIP descriptor was inverted because of the change in the priority of the groups.

Table 3. Selected results for the Pd-catalyzed allylic substitution of **S2** using the P,N ligand library **L1–L15a–h**.[a]

Entry	Ligand	H-Nu = H-CH(COOMe)$_2$ Conv [%] (t [h])[b]	H-Nu = H-CH(COOMe)$_2$ *ee* [%][c]	H-Nu = H-NHCH$_2$Ph Conv [%] (t [h])[b]	H-Nu = H-NHCH$_2$Ph *ee* [%][c]
1[d]	**L1a**	100 (24)	55 (*R*)	89 (36)	54 (*R*)
2	**L2a**	100 (24)	9 (*R*)	43 (36)	11 (*R*)
3[d]	**L6a**	100 (18)	88 (*R*)	100 (36)	85 (*R*)
4	**L6b**	100 (18)	87 (*R*)	100 (36)	86 (*R*)
5[d]	**L6c**	100 (18)	91 (*R*)	100 (36)	90 (*R*)
6	**L6d**	100 (18)	91 (*R*)	100 (36)	92 (*R*)
7	**L6g**	100 (24)	58 (*R*)	100 (36)	59 (*R*)
8	**L6h**	100 (24)	91 (*R*)	100 (36)	90 (*R*)
9	**L7a**	100 (18)	81 (*R*)	100 (36)	80 (*R*)
10[d]	**L8a**	100 (18)	91 (*R*)	100 (36)	91 (*R*)
11[d]	**L8c**	100 (18)	95 (*R*)	100 (36)	93 (*R*)
12	**L9a**	87 (24)	81 (*R*)	53 (36)	82 (*R*)
13	**L10a**	100 (18)	85 (*S*)	100 (36)	88 (*S*)
14	**L11a**	100 (24)	87 (*R*)	100 (36)	85 (*R*)
15	**L12a**	100 (24)	85 (*R*)	100 (36)	83 (*R*)
16	**L13a**	100 (18)	60 (*R*)	100 (36)	66 (*R*)
17[d]	**L14a**	100 (18)	80 (*R*)	100 (36)	83 (*R*)
18[d]	**L15a**	100 (18)	4 (*S*)	100 (36)	7 (*S*)

[a] All reactions were run at room temperature. 1 mol% [PdCl(η^3-C_3H_5)]$_2$. L/Pd = 1.1. CH_2Cl_2 as solvent. [b] Conversion percentage determined by ^{1}H NMR. [c] Enantiomeric excesses determined by ^{1}H NMR using [Eu(hfc)$_3$]. Absolute configuration in parentheses. [d] Isolated yields of **47** and **48** were >94%.

Allylic substitution of* rac-*1,3-dimethyl-3-acetoxyprop-1-ene (S3) using dimethyl malonate and benzylamine as nucleophiles [Eq. (1)]: We evaluated the phosphite–oxazoline/oxazine ligand library **L1**–**L15a**–**h** in the allylic substitution of the linear substrate **S3** [Eq. (1), R = Me, X = OAc]. This substrate is less sterically demanding than substrates **S1** and **S2**, which we used before. Enantioselectivity for **S3** is therefore more difficult to control than with hindered substrates such as **S1**. If *ee* values are to be high, the ligand must create a small chiral pocket (the chiral cavity in which the allyl is embedded) around the metal center, mainly because of the presence of less sterically demanding methyl *syn* substituents.[1] There are therefore fewer successful catalyst systems for the Pd-catalyzed allylic substitution of this substrate than for the allylic substitution of hindered substrates such as **S1**.[13]

Preliminary investigations into the solvent and ligand-to-palladium ratio revealed a different trend in solvent effect than with the previously tested substrates **S1** and **S2**. Selectivities and activities were best when THF was used and the ligand-to-palladium ratio was 1.1 (see Supporting Information).

The results of using the phosphite–oxazoline/oxazine ligand library **L1**–**L15a**–**h** in the optimized conditions are shown in Table 4. Activities and enantioselectivities were also high (*ee* up to 84%) in the substitution of **S3** using the Pd/**L12e** catalyst system. Activities followed the same trends as for the substitution of substrates **S1** and **S2** and were mainly affected by the substituents in the oxazoline, in the alkyl backbone chain and in the biaryl phosphite moiety. Reaction rates were therefore best with ligands containing less sterically hindered oxazoline substituents, methyl substituents in the alkyl backbone chain and bulky substituents in the *ortho* positions of the biaryl moieties (TOF's up to 120 mol **S2** × (mol Pd × h)$^{-1}$).

Enantioselectivities were again affected by the substituents at the oxazoline and at the alkyl backbone chain, the presence of a second stereogenic center in the oxazoline ring, the size of the heterocycle and the substituents/configurations in the biaryl phosphite moiety. However, the effects of the substituent/configuration of the alkyl backbone chain and of the biaryl phosphite group were different from those observed in the substitution of **S1** and **S2**. Unlike the substitution of **S1** and **S2**, therefore, replacing the methyl substituents (ligands **L6**–**L10**) with phenyls (**L11**–**L12**) in the alkyl backbone chain considerably increases enantioselectivities (Table 4, entries 6 and 15 vs 20 and 21). Also, the change in the configuration of the alkyl backbone chain produces the preferential formation of the opposite enantiomer of the substitution products. In contrast with the substitution of **S1** and **S2**, however, the *ee* values are different (Table 4, entries 6 vs 19). Finally, with regard to the effect of the configuration/substituents of the biaryl phosphite moiety on enantioselectivity, we found two main trends: a) using unsubstituted biaryl moieties is advantageous in terms of enantioselectivity (Table 4, entries 6–13) and b) there is a cooperative effect between the configuration of the biaryl moieties and the alkyl backbone chain that results in a matched combination for ligands containing an *S*-binaphthyl phosphite moiety (Table 4, entry 10 and 12 vs 11 and 13). Interestingly, and unlike the substitution of **S1** and **S2**, this cooperative effect is highly advantageous as enantioselectivities increased from 64 to 72% (Table 4, entries 9 vs 10).

Table 4. Selected results for the Pd-catalyzed allylic substitution of **S3** using the P,N ligand library **L1**–**L15a**–**h**.[a]

Entry	Ligand	H-Nu = H-CH(COOMe)$_2$ Conv [%] (t [min])[b]	*ee* [%][c]	H-Nu = H-NHCH$_2$Ph Conv [%] (t [h])[b]	*ee* [%][c]
1	**L1a**	85 (120)	15 (*R*)	100 (24)	17 (*R*)
2	**L2a**	22 (120)	0	49 (24)	0
3	**L3a**	84 (120)	16 (*R*)	100 (24)	17 (*R*)
4	**L4a**	67 (120)	7 (*R*)	100 (24)	9 (*R*)
5	**L5a**	43 (120)	0	63 (24)	0
6[e]	**L6a**	100 (90)	39 (*R*)	100 (18)	41 (*R*)
7[e]	**L6b**	100 (90)	25 (*R*)	100 (18)	27 (*R*)
8[e]	**L6c**	100 (90)	32 (*R*)	100 (18)	33 (*R*)
9	**L6d**	100 (120)	64 (*R*)	100 (18)	65 (*R*)
10	**L6e**	93 (120)	72 (*R*)	100 (18)	71 (*R*)
11	**L6f**	72 (120)	13 (*R*)	100 (18)	18 (*R*)
12	**L6g**	100 (120)	58 (*R*)	100 (18)	62 (*R*)
13	**L6h**	98 (120)	29 (*R*)	100 (18)	28 (*R*)
14	**L7a**	100 (120)	47 (*R*)	100 (18)	58 (*R*)
15[e]	**L8a**	100 (120)	57 (*R*)	100 (18)	59 (*R*)
16	**L8c**	100 (120)	28 (*R*)	100 (18)	27 (*R*)
17	**L8e**	48 (120)	59 (*R*)	100 (24)	61 (*R*)
18	**L9a**	98 (120)	47 (*R*)	100 (24)	49 (*R*)
19	**L10a**	100 (90)	23 (*S*)	100 (18)	26 (*S*)
20	**L11a**	95 (120)	60 (*R*)	100 (18)	62 (*R*)
21	**L12a**	62 (120)	76 (*R*)	86 (24)	77 (*R*)
22	**L12e**	34 (120)	79 (*R*)	67 (24)	79 (*R*)
23[e]	**L13a**	100 (120)	19 (*R*)	100 (18)	21 (*R*)
24	**L14a**	100 (120)	34 (*R*)	100 (18)	29 (*R*)
25	**L15a**	76 (120)	24 (*S*)	100 (18)	22 (*S*)
26[d]	**L6e**	8 (120)	81 (*R*)	–	–
27[d]	**L12e**	14 (240)	84 (*R*)	–	–

[a] All reactions were run at room temperature. 0.5 mol% [PdCl(η^3-C_3H_5)]$_2$. THF as solvent. 1.1 mol% ligand. [b] Conversion measured by GC. Reaction time shown in parentheses. [c] Enantiomeric excesses measured by GC. The absolute configuration appears in parentheses. [d] T = −10 °C. [e] Isolated yields of **49** and **50** were > 92%.

Enantioselectivities (up to 84%) were therefore best for ligand **L12e**, which has an electron-withdrawing substituent in the oxazoline, phenyl substituents in the alkyl backbone chain and an *S*-binaphthyl phosphite moiety. These results, which clearly show the efficiency of using highly modular scaffolds in the ligand design, are among the best reported for this type of unhindered substrates.[13]

Allylic alkylation of cyclic substrates [Eq. (2)]: With regard to the unhindered substrate **S3**, enantioselectivity in cyclic substrates is difficult to control, mainly because of the presence of less sterically *anti* substituents. These *anti* substituents are thought to play a crucial role in the enantioselection observed with cyclic substrates in the corresponding Pd–allyl intermediate.[1]

In this section we show that the chiral phosphite–oxazoline/oxazine ligand library **L1**–**L15a**–**h** applied above to the Pd-catalyzed allylic substitution of linear substrates (**S1**–**S3**)

can also be used for cyclic substrates (*ee* up to 83%). We tested two cyclic substrates (equation 2): *rac*-3-acetoxycyclohexene **S4** (which is widely used as a model substrate) and *rac*-3-acetoxycycloheptene **S5**.

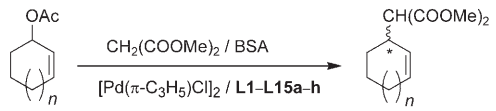

(2)

S4: *n*=1
S5: *n*=2

51: *n*=1
52: *n*=2

Preliminary investigations into the solvent effect and ligand-to-palladium ratio showed the same trends as with the previously tested unhindered linear substrate **S3**. The trade-off between enantioselectivities and reaction rates was therefore optimum with tetrahydrofuran and a ligand-to-palladium ratio of 1.1 (see Supporting Information).

The results of using the phosphite-oxazoline/oxazine ligand library **L1**–**L15a**–**h** under the optimized conditions are shown in Table 5. We also obtained high activities and enantioselectivities (up to 83%) in the alkylation of cyclic substrates **S4** and **S5**.

In general, activities followed the same trends as for the substitution of substrates **S1**–**S3** and were mainly affected by the substituents in the oxazoline, in the alkyl backbone chain and in the biaryl phosphite moiety. The reaction rates were therefore best with ligands containing less sterically hindered oxazoline substituents, methyl substituents in the alkyl backbone chain and bulky substituents in the *ortho* positions of the biaryl moieties (TOF's > 100 mol substrate $\times$ (mol Pd $\times$ h)$^{-1}$).

Table 5. Selected results for the Pd-catalyzed allylic substitution of **S4** and **S5** using the P,N ligand library **L1**–**L15a**–**h**.[a]

Entry	Ligand	**S4** Conv [%] (t [min])[b]	**S4** *ee* [%][c]	**S5** Conv [%] (t [h])[b]	**S5** *ee* [%][c]
1[d]	**L1a**	36 (120)	5 (*R*)	48 (12)	8 (*R*)
2	**L2a**	13 (120)	0	22 (12)	2 (*R*)
3	**L3a**	35 (120)	7 (*R*)	46 (12)	7 (*R*)
4	**L4a**	18 (120)	0	29 (12)	0
5	**L5a**	15 (120)	0	29 (12)	0
6[d]	**L6a**	88 (90)	42 (*R*)	100 (12)	46 (*R*)
7	**L6b**	46 (120)	58 (*R*)	79 (12)	62 (*R*)
8[d]	**L6c**	50 (120)	60 (*R*)	67 (12)	66 (*R*)
9	**L6d**	5 (120)	0	16 (12)	0
10	**L6e**	8 (120)	35 (*S*)	29 (12)	42 (*S*)
11	**L6f**	9 (120)	25 (*R*)	37 (12)	28 (*R*)
12[d]	**L6g**	42 (120)	70 (*S*)	76 (12)	75 (*S*)
13	**L6h**	58 (120)	58 (*R*)	85 (12)	61 (*R*)
14	**L7a**	95 (120)	36 (*R*)	100 (12)	39 (*R*)
15[d]	**L8a**	85 (120)	55 (*R*)	100 (12)	56 (*R*)
16	**L8c**	9 (120)	54 (*R*)	26 (12)	52 (*R*)
17	**L8e**	9 (120)	68 (*R*)	31 (12)	71 (*R*)
18	**L8g**	21 (120)	75 (*R*)	41 (12)	83 (*R*)
19[d]	**L9a**	28 (120)	57 (*R*)	45 (12)	63 (*R*)
20	**L10a**	79 (120)	37 (*S*)	100 (12)	42 (*S*)
21	**L11a**	14 (120)	6 (*S*)	56 (12)	11 (*S*)
22[d]	**L12a**	8 (120)	7 (*S*)	23 (12)	11 (*S*)
23	**L13a**	78 (120)	37 (*R*)	100 (12)	43 (*R*)
24	**L14a**	82 (120)	43 (*R*)	100 (12)	49 (*R*)
25[d]	**L15a**	32 (120)	13 (*R*)	67 (12)	15 (*R*)

[a] All reactions were run at room temperature. 0.5 mol% $[PdCl(\eta^3\text{-}C_3H_5)]_2$. THF as solvent. 1.1 mol% ligand. [b] Conversion measured by GC. Reaction time shown in parentheses. [c] Enantiomeric excesses measured by GC. The absolute configuration appears in parentheses. [d] Isolated yields >93% based on recovered starting material.

Again, enantioselectivities were affected by the substituents at the oxazoline and at the alkyl backbone chain, the presence of a second stereogenic center in the oxazoline ring, the size of the heterocycle and the substituents/configuration in the biaryl phosphite moiety. However, the effects of the substituent of the alkyl backbone chain and biaryl phosphite group were different from those observed in the alkylation of **S1**–**S3**. Therefore, unlike in the alkylation of **S1**–**S3**, replacing the methyl substituents (ligands **L6**–**L10**) by phenyls (**L11**–**L12**) in the alkyl backbone chain considerably decreased enantioselectivities (Table 5, entries 6 and 15 vs 20 and 21). With regard to the effect of the substituents of the biaryl phosphite moiety on enantioselectivity, and in contrast to the alkylation of **S3**, we found that bulky trimethylsilyl substituents in the *ortho* positions are needed if enantioselectivities have to be high (Table 5, entries 6–13). Also, the cooperative effect between the configuration of the biaryl moiety and the alkyl backbone chain resulted in a matched combination for ligand **L6g**, which contains an *ortho*-disubstituted trimethylsilyl *S*-binaphthyl phosphite group.

Enantioselectivities (up to 83%) were therefore best for ligand **L8g**, which contains the optimal combination of ligand parameters (an electron-withdrawing substituent in the oxazoline, methyl substituents in the alkyl backbone chain and *ortho*-substituted trimentylsilyl *S*-binaphthyl phosphite moiety). These results, which again clearly show the efficiency of highly modular scaffolds in the ligand design, are among the best reported for this type of unhindered substrates.[5,7b,13a,14]

Allylic substitution of monosubstituted linear substrates S6 and S7 [Eq. (3)]: Encouraged by the excellent results obtained for several disubstituted linear substrates and cyclic substrates, we examined the regio- and stereoselective allylic alkylation of 1-(1-naphthyl)allyl acetate (**S6**) and 1-(1-naphthyl)-3-acetoxyprop-1-ene (**S7**) with dimethyl malonate as nucleophile [Eq. (3)]. For these substrates, not only does the enantioselectivity of the process need to be controlled but regioselectivity is also a problem because a mixture of regioisomers can be obtained. Most Pd catalysts developed to date favour the formation of achiral linear product **54** rather than the desired branched isomer **53**.[15] The development of highly regio- and enantioselective Pd catalysts is therefore still a challenge.[5,8,9b,16] Because of the high π-acceptor ability of the biaryl phosphite moiety in ligands **L1**–**L15a**–**h**, we expected to enhance the S_N1 character of the nucleophilic attack that would favour the formation of the branched isomer.[8]

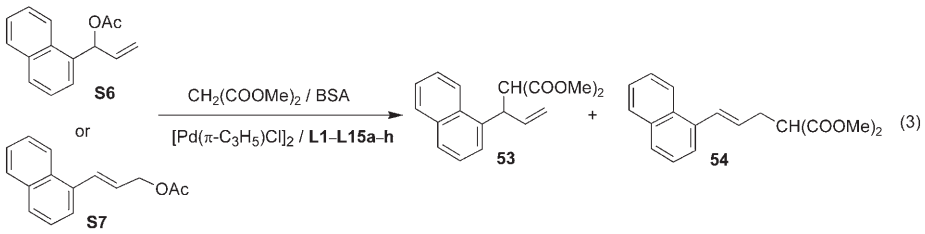

The results obtained with the phosphite–oxazoline/oxazine ligand library **L1–L15a–h** are summarized in Table 6. High activities and enantioselectivities up to 95% combined with regioselectivities >95% in favour of the branched product **53** were obtained, under standard reaction conditions, with the Pd/**L6g** and Pd/**L8h** catalyst systems. The results indicated that the trade-off between regio- and enantioselectivities was best for ligands that contain an electron-withdrawing aryl substituent in the oxazoline moiety, methyl substituents in the alkyl backbone chain and an *ortho*-substituted trimethylsilyl binaphthyl phosphite group. Ligands **L6g** and **L8h** therefore produced the desired branched isomer **53** as the major product with high regio- and enantioselectivity (Table 6, entries 12 and 18). Interestingly, the absolute configuration of the biaryl moiety seems to control the absolute configuration of the stereochemical outcome. Therefore, both enantiomers of the product can be obtained in high regio- and enantioselectivities simply by changing the configuration of the biaryl moiety (Table 6, entries 12, 13 and 18). These results are among the best reported for this type of substrates.[5,8,16]

Table 6. Selected results for the Pd-catalyzed allylic alkylation of monosubstituted substrate **S6** and **S7** using the ligand library **L1–L15a–h** under standard conditions[a]

Entry	Ligand	Substrate	Conv [%][b] (t [min])	**53**/**54**[c]	*ee* [%][d]
1	**L1a**	**S6**	100 (120)	50/50	14 (*S*)
2	**L2a**	**S6**	100 (120)	25/75	4 (*S*)
5	**L5a**	**S6**	100 (120)	20/80	4 (*S*)
6	**L6a**	**S6**	100 (60)	85/15	76 (*S*)
7	**L6b**	**S6**	100 (60)	65/35	82 (*S*)
8	**L6c**	**S6**	100 (60)	85/15	93 (*S*)
9[e]	**L6d**	**S6**	100 (120)	>95/<5	74 (*R*)
12[e]	**L6g**	**S6**	100 (60)	>95/<5	94 (*R*)
13	**L6h**	**S6**	100 (60)	80/20	90 (*S*)
14	**L7a**	**S6**	100 (60)	80/20	60 (*S*)
15	**L8a**	**S6**	100 (60)	85/15	84 (*S*)
16	**L8c**	**S6**	100 (60)	85/15	95 (*S*)
17	**L8e**	**S6**	100 (120)	80/20	88 (*S*)
18[e]	**L8h**	**S6**	100 (60)	95/5	95 (*S*)
19	**L9a**	**S6**	100 (120)	80/20	61 (*S*)
20	**L11a**	**S6**	100 (120)	60/40	89 (*S*)
21	**L12a**	**S6**	100 (120)	65/35	94 (*S*)
22	**L13a**	**S6**	100 (60)	85/15	72 (*S*)
23	**L15a**	**S6**	100 (60)	65/35	33 (*S*)
24[e]	**L6g**	**S7**	100 (60)	>95/<5	93 (*R*)
25[e]	**L8h**	**S7**	100 (60)	95/5	96 (*S*)

[a] All reactions were run at room temperature. 1 mol% $[PdCl(\eta^3\text{-}C_3H_5)]_2$. Dichloromethane as solvent. 2.2 mol% ligand. [b] Reaction time in minutes shown in parentheses. [c] Percentage of branched (**53**) and linear (**54**) isomers. [d] Enantiomeric excesses determined by HPLC. The absolute configuration appears in parentheses. [e] Isolated yields of **53** were >93%.

Origin of enantioselectivity—Study of the Pd–π-allyl intermediates: To provide further insight into how ligand parameters affect catalytic performance, we studied the Pd–π-allyl compounds **55–62**, $[Pd(\eta^3\text{-allyl})(L)]BF_4$ (L = phosphite–oxazoline ligands), since they are key intermediates in the allylic substitution reactions studied.[1] These ionic palladium complexes, which contain 1,3-diphenyl, 1,3-dimethyl or cyclohexenyl allyl groups, were prepared using the previously described method from the corresponding Pd–allyl dimer and the appropriate ligand in the presence of silver tetrafluoroborate (Scheme 3).[17] The complexes were characterized by elemental analysis and by ^1H, ^{13}C and ^{31}P NMR spectroscopy. The spectral assignments (see Experimental Section) were based on information from ^1H–^1H, ^{31}P–^1H and ^{13}C–^1H correlation measurements in combination with ^1H–^1H NOESY experiments. Unfortunately, we were unable to obtain any crystal of sufficient quality to perform X-ray diffraction measurements.

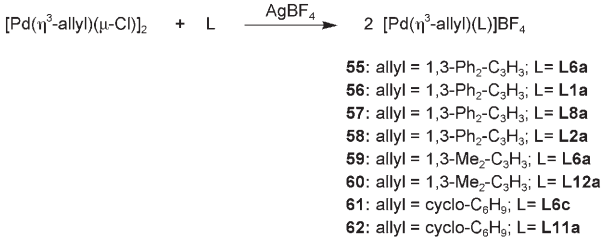

Scheme 3. Preparation of $[Pd(\eta^3\text{-allyl})(L)]BF_4$ complexes **55–62**.

Palladium 1,3-diphenyl–allyl complexes: When the phosphite–oxazoline/oxazine ligand library **L1–L15a–h** was used in the allylic substitution of disubstituted hindered substrates **S1** and **S2**, the catalytic results indicated that the substituent of the oxazoline and of the alkyl backbone chain had an important effect on enantioselectivity, while the substituents/configurations of the biaryl phosphite moiety and the presence of a second sterogenic center in the oxazoline ring had less significant effects. An electron-withdrawing substituent (4-CF_3-Ph) in the oxazoline moiety and methyl groups in alkyl backbone chain are therefore required if enantioselectivity is to be high. To understand this catalytic behaviour, we studied Pd–π-allyl complexes **55–58**, which contain ligands **L6a, L1a**, **L8a** and **L2a**, respectively.

With complexes $[Pd(\eta^3\text{-}1,3\text{-diphenylallyl})(\mathbf{L6a})]BF_4$ (**55**) and $[Pd(\eta^3\text{-}1,3\text{-diphenylallyl})(\mathbf{L1a})]BF_4$ (**56**), we studied the effect of the substituents of the alkyl backbone chain. These complexes maintain the same substituent in the oxazoline moiety but have different substituents in the alkyl backbone chain. Therefore, while ligand **L6a**, which contains methyl substituents at the alkyl backbone chain, provided good

enantioselectivity (*ee* up to 84% (*S*)), ligand **L1a**, which does not have substituents in this position, was less enantioselective (*ee* up to 52% (*S*)). On the other hand, by comparing the Pd study of complexes **55** and **56** with complexes [Pd(η^3-1,3-diphenylallyl)(**L8a**)]BF_4 (**57**) and [Pd(η^3-1,3-diphenylallyl)(**L2a**)]BF_4 (**58**), respectively, we studied how the electron and steric properties of the oxazoline substituent affect catalytic performance. Pd/**L8a**, which contains an electron-withdrawing substituent, provided the highest enantioselectivity (*ee* up to 90% (*S*)), while Pd/**L2a** which has a bulky substituent in the oxazoline moiety, provided the lowest enantioselectivity (*ee* up to 14% (*S*)).

The VT-NMR (30 to −80°C) study of Pd–allyl intermediate **55**, which contains ligand **L6a**, had a mixture of two isomers in equilibrium in a ratio of 1.5:1 (see Experimental Section).[18] Both isomers were unambiguously assigned by NMR (^{1}H, ^{31}P, ^{13}C, ^{1}H–^{1}H, ^{1}H–^{13}C and ^{1}H–^{31}P correlation and NOESY experiments) to the two *syn*/*syn endo* **A** and *exo* **B** isomers (Scheme 4). In both isomers, the NOE indicates interactions between both terminal protons of the allyl group and also between the central allyl proton with *ortho* hydrogens of both phenyl groups of the allyl ligand, which clearly indicates a *syn*/*syn* disposition (Figure 4). Moreover, one of the terminal allyl protons of the major isomer **A** shows a NOE interaction with the *ortho* hydrogen of the phenyl-oxazoline substituent. In addition, one of the methyl substituents of the alkyl backbone chain shows a NOE contact with the central allyl proton in isomer **A**, while in **B** isomer this interaction appears with one of the terminal allyl protons. Such interactions can be explained by assuming a *syn*/*syn endo* disposition for isomer **A** and a *syn*/*syn exo* disposition for isomer **B** (Figure 4). This assignment is also in agreement with the shift to higher fields in isomer **A** of the terminal allylic proton and carbon signals close to the oxazoline moiety, with respect to the corresponding signals for isomer **B**. This is due to the shielding effect of the phenyl oxazoline ring.[19] For both isomers, the carbon NMR chemical shifts indicate that the more electrophilic allyl carbon terminus is *trans* to the phosphite moiety. Assuming that the nucleophilic attack takes place at the more electrophilic allyl carbon terminus[1] and on the basis of the observed stereochemical outcome of the reaction (84% (*S*) in product **45**), and as the enantiomeric excess of alkylation product **45** differs from the diastereoisomeric excess (*de* 20% (*R*)) of the Pd-intermediates, the **B** isomer must react faster than the **A** isomer. To prove this we also studied the reactivity of the Pd-intermediates with sodium malonate at low temperature by in situ NMR (Figure 5). Our results show that the minor isomer **B** reacts around 15 times faster than isomer **A**. If we take into account the relative reaction rates and the abundance of both isomers, the calculated ee should be 82%, which matches the ee obtained experimentally.[20] We can therefore conclude that the nucleophilic attack takes place predominantly at the allyl terminus *trans* to the phosphite moiety of the minor **B** Pd-intermediate. This is also consistent with the fact that, for both isomers, the most electrophilic allylic terminal carbon atom is the one *trans* to the phosphite in the minor **B** isomer.

The VT-NMR study of Pd–allyl intermediate **56**, which contains ligand **L1a**, also had a mixture of two *syn*/*syn endo*

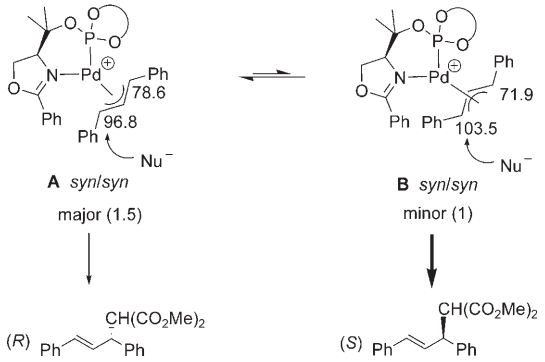

Scheme 4. Diastereoisomer Pd–allyl intermediates for **S1** with ligand **L6a**. The relative amounts of each isomer are drawn in parenthesis. The chemical shifts (in ppm) of the allylic terminal carbons are shown.

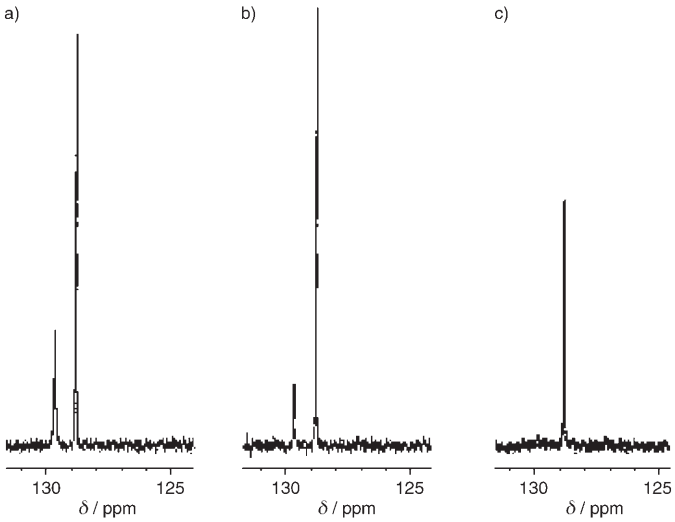

Figure 5. ^{31}P{^{1}H NMR spectra of [Pd(η^3-1,3-diphenylallyl)(**L6a**)]BF_4 (**55**) in CD_2Cl_2 at −60°C a) before the addition of sodium malonate; b) after the addition of sodium malonate and c) 5 min after the addition of sodium malonate.

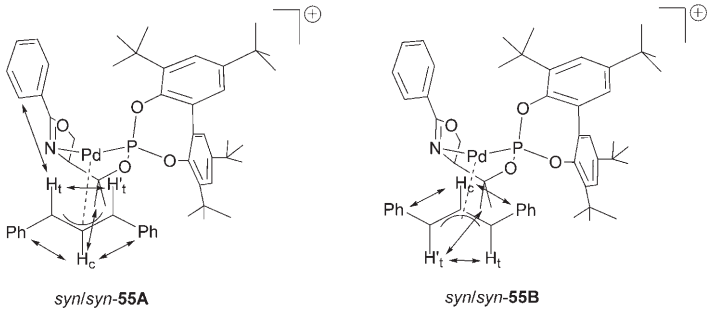

Figure 4. Relevant NOE contacts from NOESY experiment of [Pd(η^3-1,3-diphenylallyl)(**L6a**)]BF_4 (**55**) isomers.

(**A**) and *exo* (**B**) isomers but in a ratio of 5.6:1, respectively (see Experimental Section). Also, the more electrophilic allyl carbon terminus was *trans* to the phosphite moiety (Scheme 5). Again, on the basis of the stereochemical out-

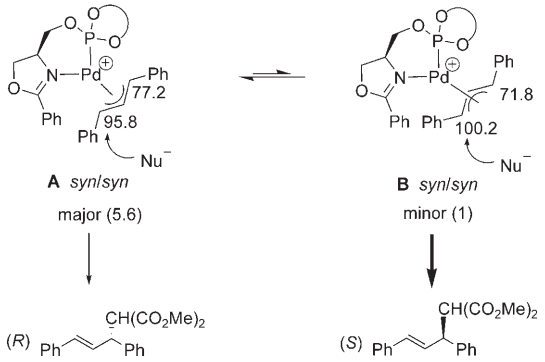

Scheme 5. Diastereoisomer Pd-allyl intermediates for **S1** with ligand **L1a**. The relative amounts of each isomer are drawn in parenthesis. The chemical shifts (in ppm) of the allylic terminal carbons are shown.

come of the reaction, which was 52% (*S*) in product **45**, and the fact that the enantiomeric excess of alkylation product **45** differs from the diastereoisomeric excess (*de* 69% (*R*)) of the Pd intermediates, the **B** isomer must react faster than the **A** isomer. This is also consistent with the fact that, for both isomers, the most electrophilic allylic terminal carbon atom is the one *trans* to the phosphite in the minor **B** isomer. The lower enantioselectivity with this system than with the previous Pd/**L6a** catalytic system can be attributed to the decrease in the relative amount of isomer **B** with respect to isomer **A** compared with the population of isomers (**A** and **B**) for complex **55**. Our study of the models[21] indicated that replacing the methyl substituents (ligand **L6a**, complex **55**) by hydrogen substituents (ligand **L1a**, complex **56**) in the ligand's alkyl backbone chain produces a change in the spatial disposition of the phosphite moiety. This causes the upper phenyl fragment of the phosphite group to bend towards the region in which the substrate is coordinated. This creates a greater steric interaction between the *tert*-butyl groups of the phosphite moiety and one of the phenyl groups of the substrate in the **B** isomer of complex **56** than in complex **55** (Figure 6), which justifies the preferential formation of isomer **A** in complex **56** compared to complex **55**.

The VT-NMR study of Pd–allyl intermediate **57**, which contains ligand **L8a**, had also a mixture of two *syn*/*syn endo* (**A**) and *exo* (**B**) isomers in a ratio of 1:1.5, respectively (Scheme 6). Unlike complex **55**, the greatest amount of species corresponds to isomer **B**. Again, the carbon NMR chemical shifts indicate that the most electrophilic allyl carbon terminus is *trans* to the phosphite moiety in the **B** isomer. The fact that this catalytic system provides better enantiosectivities than Pd/**L6a** (**55**) must be due to the greater amount of the most reactive **B** isomer in complex **57**.

The VT-NMR study of Pd–1,3-diphenyl allyl intermediate **58**, which contains ligand **L2a**, indicated the presence of a

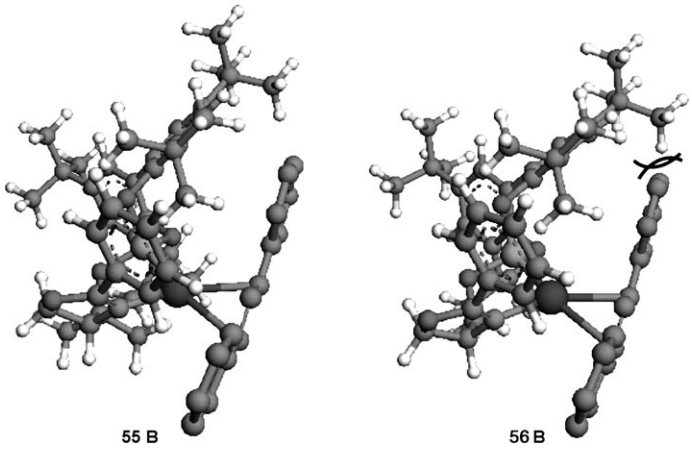

Figure 6. Pd-allyl intermediates **55B** and **56B**. H atoms in the allyl ligand are omitted for clarity.

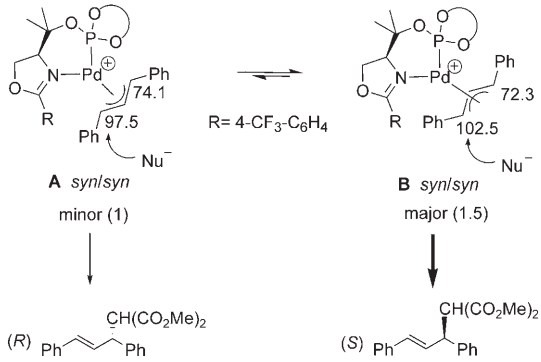

Scheme 6. Diastereoisomer Pd–allyl intermediates for **S1** with ligand **L8a**. The relative amounts of each isomer are drawn in parenthesis. The chemical shifts (in ppm) of the allylic terminal carbons are shown.

mixture of three species in a ratio of 15:3:1 (see Experimental Section). The major **A** and the minor **B** isomers were assigned by NOE to the *syn*/*syn endo* and *exo* isomers, while compound **C** was attributed to the species that contains two ligands coordinated in a monodentated fashion (Scheme 7). The formation of compound **C** was confirmed by adding an

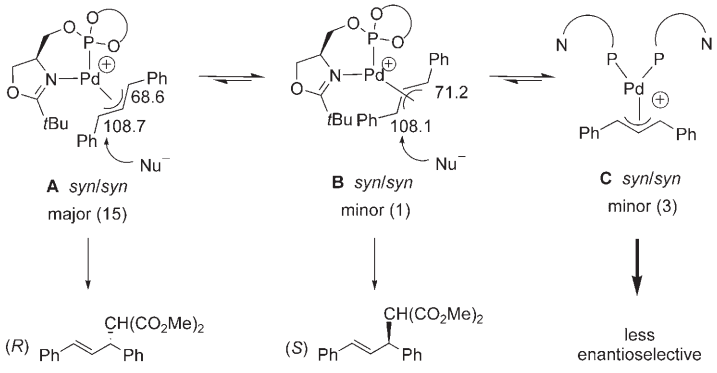

Scheme 7. Diastereoisomer Pd–allyl intermediates for **S1** with ligand **L2a**. The relative amounts of each isomer are drawn in parenthesis. The chemical shifts (in ppm) of the allylic terminal carbons are shown.

excess of ligand, which resulted in an increase in the amount of species **C** present in solution. In comparison with complex **56**, which contains ligand **L1a**, we found that the relative amount of isomer **A** with respect to **B** increased. Our study of the models[21] indicated that replacing a phenyl substituent in the oxazoline group (ligand **L1a**, complex **56**) by a bulky *tert*-butyl substituent (ligand **L2a**, complex **58**) produces a different spatial arrangement around the metal center. This causes an increase of the previous steric interaction observed on **56**, between one of the *tert*-butyl phosphite group and one of the phenyl substituents of **S1**, and also generates a new steric interaction between the *tert*-butyl oxazoline group and the other phenyl substituents of **S1** on the **B** isomer, so the formation of the **A** isomer is more favourable (Figure 7). Another important difference between com-

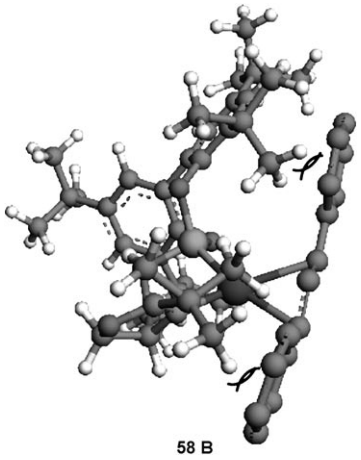

Figure 7. Pd–allyl intermediate **58B**. H atoms in the allyl ligand are omitted for clarity.

plexes **56** and **58** is the lower electron differentiation between the more electrophilic allylic terminus carbon atoms of both isomers (**A** and **B**) in complex **58** ($\Delta(\delta^{13}C) \approx 0.6$ ppm) than in complex **56** ($\Delta(\delta^{13}C) \approx 4.4$ ppm). This low electron differentiation in complex **58** suggests that the nucleophile can attack both isomers (**A** and **B**) at a similar rate. However, the difference between the diastereoisomeric ratio and enantioselectivity observed in the alkylation of **S1** (*de* 87% (*R*) vs *ee* 14% (*S*)) suggests that another cause is responsible for the main catalytic performance. Therefore, the fact that enantioselectivity when the Pd/**L2a** catalyst was used (*ee* up to 14%) was lower than when the Pd/**L1a** catalyst was used (*ee* up to 52%) may be due to the presence of Pd-complex **C**. This type of complexes are known to be faster and less enantioselective than their bidentate counterparts.[22]

In summary, our study of the allyl intermediate indicates that changes in the substituents of the alkyl backbone chain and electronic properties of the oxazoline substituents lead to changes in the ratio of the species that provide both enantiomers of alkylation product **45**. Also, an increase in the bulkiness of the oxazoline substituents led to the formation of species with ligands coordinated in monodentated fashion.

Palladium–1,3-dimethylallyl complexes: When the phosphite-oxazoline ligand library **L1**–**L15a**–**h** was used in the allylic substitution of unhindered linear **S3** substrate, the catalytic results revealed a different trend for the effect of the substituents of the alkyl backbone chain than with the previously hindered substrates **S1** and **S2**. Replacing the methyl substituents by phenyls in the alkyl backbone chain had a considerably positive effect on enantioselectivity. To understand this catalytic behaviour, we studied Pd–π-allyl complexes **59** and **60**, which contain ligands **L6a** and **L12a**, respectively. While ligand **L12a**, which contains phenyls substituents at the alkyl backbone chain, provided high enantioselectivities (Table 4, entry 21, *ee* up to 77%), ligand **L6a**, which contains methyl substituents, was less enantioselective (Table 4, entry 6, *ee* up to 41%).

For both Pd–1,3-dimethyl allyl intermediates **59** (**L6a**) and **60** (**L12a**), the study of the VT-NMR (35 to −80 °C) indicated the presence of a mixture of two isomers (**A** and **B**) at a ratio of 1:1 (see Experimental Section). All species were assigned by NOE to the *syn*/*syn exo* and *endo* isomers (Scheme 8). For both complexes, the NOE indicates interactions between both terminal protons of the allyl group and also between the central allyl proton with methyl protons of the allyl ligand, which clearly indicates a *syn*/*syn* disposition for all the isomers. Moreover, one of the methyl protons of the allyl ligand of the isomers **B** shows a NOE interaction with the *ortho* hydrogen of the phenyl-oxazoline substituent. Such interactions can be explained by assuming a *syn*/*syn exo* disposition for isomers **B** (Scheme 8). This assignment is also in agreement with the shift to higher fields in isomers **A** of the terminal allylic proton and carbon signals close to the oxazoline moiety, with respect to the corresponding signals for isomers **B**. This is due to the shielding effect of the phenyl-oxazoline ring.[19] As for the previous 1,3-diphenylallyl intermediates, the NMR data indicate that the more electrophilic allyl terminal carbon is *trans* to the phosphite moiety at the **B** isomers (**59B** and **60B**). However, since isomers **59A** and **59B** show the same population and electronic properties at the allyl fragment as isomers **60A** and **60B** (Scheme 8), respectively, the difference in enantioselectivity observed between Pd/**L6a** and Pd/**L12a** catalysts cannot be explained by the reactivity of the nucleophile *versus* the different π-allyl intermediates.

A plausible explanation can be found either in the enhancement of the steric interaction upon attack of the nucleophile as the result of the formation of a more bulky chiral pocket or a late transition state.[1] Nucleophilic substitution of the (π-allyl)Pd cationic complex to form the Pd–olefin complex must be accompanied by rotation.[1] The study of the models (Schemes 9 and 10) indicates that for Pd-intermediate **60**, the rotation is more favoured in the **60A** isomer (which would lead to the formation of the (*R*)-**49** enantiomer) because the rotation in the **60B** isomer led to an extra unfavourable steric interaction between the methyl substitu-

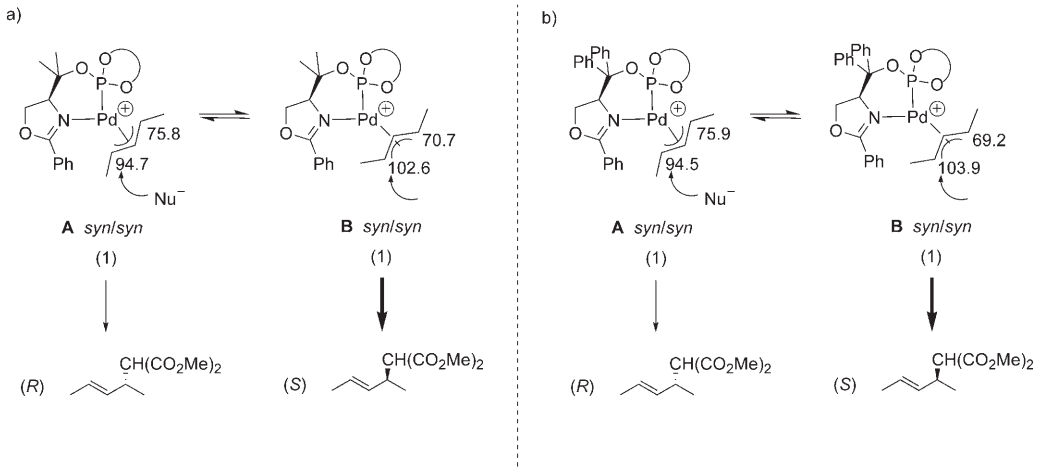

Scheme 8. Diastereoisomer Pd–allyl intermediates a) **59** for **S3** with ligand **L6a** and b) **60** for **S3** with ligand **L12a**. The relative amounts of each isomer are drawn in parenthesis. The chemical shifts (in ppm) of the allylic terminal carbons are shown.

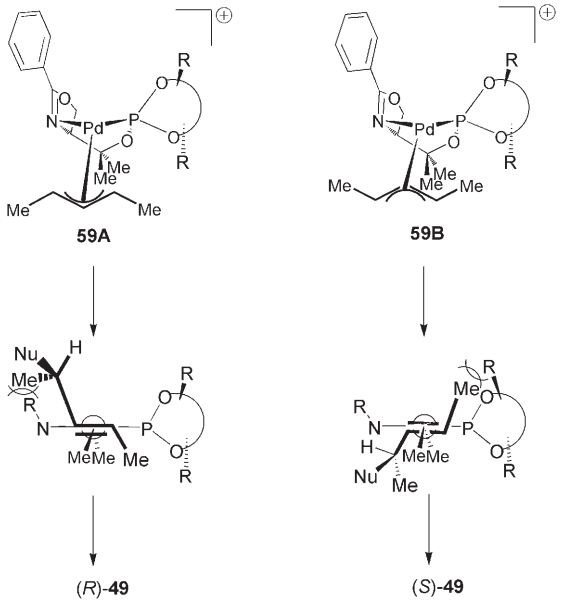

Scheme 9. Steric interaction upon attack of the nucleophile in Pd-intermediate **59**.

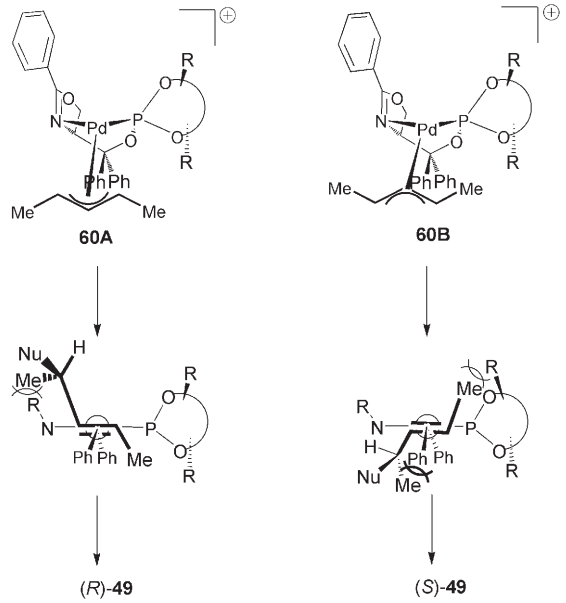

Scheme 10. Steric interaction upon attack of the nucleophile in Pd-intermediate **60**.

ent of the olefin and one of the phenyls of the alkyl backbone chain (Scheme 10). However, for complex **59**, there is no such interaction between the methyl substituents of the alkyl chain and the methyl substituent of the olefin in the **59B** isomer and explain its low enantioselectivity.

Palladium–1,3-cyclohexenylallyl complexes: When the phosphite–oxazoline ligand library **L1**–**L15a**–**h** was used in the allylic substitution of cyclic substrates **S4** and **S5**, the catalytic results showed that replacing the methyl substituents of the alkyl backbone chain by phenyls considerably decreased enantioselectivities. To understand this catalytic behaviour, we studied Pd–π-allyl complexes **61**–**62**, which contain ligands **L6c** and **L11a**. Therefore, ligand **L6c**, which contains methyl substituents at the alkyl backbone chain, provided higher enantioselectivities than ligand **L11a**, with phenyl substituents in this position.

The VT-NMR (35 to −80 °C) study of Pd–1,3-cyclohexenylallyl intermediates **61** and **62**, which contain ligands **L6c** and **L11a**, respectively, showed a mixture of the two possible isomers in a ratio of 10:90 and 40:60, respectively (see Supporting Information). All the isomers were unambiguously assigned by NOE to the **A** and **B** isomers (Scheme 11). Therefore, for isomers **61A** and **62A**, the NOE indicates interactions between the central allyl proton with one of the substituents of the alkyl backbone chain of the ligand (methyl hydrogens for complex **61** and *ortho* hydrogens of the phenyl group for complex **62**). The assign-

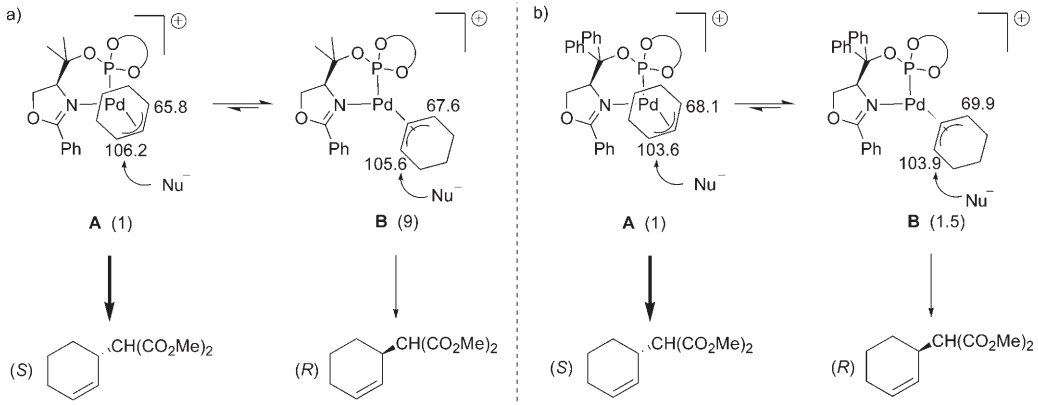

Scheme 11. Diastereoisomer Pd–allyl intermediates a) **61** for **S4** with ligand **L6c** and b) **62** for **S4** with ligand **L11a**. The relative amounts of each isomer are drawn in parenthesis. The chemical shifts (in ppm) of the allylic terminal carbons are shown.

ment was also confirmed by the presence of NOE interactions between the methylenic hydrogens of the allyl ligand and the *ortho* hydrogen of the phenyloxazoline substituent (Figure 8a). However, for isomers **61B** and **62B**, the NOE

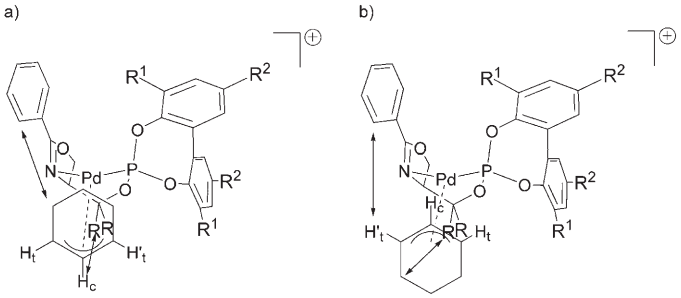

Figure 8. Relevant NOE contacts from NOESY experiment for a) isomers **A** and b) isomers **B** of complexes [Pd(η^3-1,3-cyclohexenylallyl)(**L6c**)]BF_4 (**61**; R = Me, R^1 = $SiMe_3$ and R^2 = H) and [Pd(η^3-1,3-cyclohexenylallyl)(**L11a**)]BF_4 (**62**; R = Ph, R^1 = R^2 = *t*Bu).

indicates interactions between one of the terminal allyl protons and the *ortho* hydrogen of the phenyl-oxazoline substituent and also between the methylenic hydrogens of the allyl ligand and one of the substituents of the alkyl backbone chain of the ligand (Figure 8b). For all isomers, the carbon NMR chemical shifts indicated that the most electrophilic allylic terminus carbon is *trans* to the phosphite moiety. Interestingly, the difference between the diastereoisomeric ratio and enantioselectivity observed in the alkylation of **S4** for complex **61** (*de* 80% (*R*) vs *ee* 60% (*R*)) and for complex **62** (*de* 20% (*R*) vs *ee* 6% (*S*)) indicates that in both complexes the nucleophile reacts faster with the minor **A** isomer. This was confirmed by the reactivity of the Pd intermediates of each Pd–cyclohexenylallyl complexes **61** and **62** with sodium malonate at low temperature by in situ NMR.

Conclusion

A library of phosphite-oxazoline/oxazine ligands **L1**–**L15a**–**h** has been synthesized for the Pd-catalyzed allylic substitution reactions of several substrates with different electronic and steric properties. These series of ligands have four main advantages: 1) they can be prepared efficiently from readily available hydroxyl amino acid derivatives; 2) the π-acceptor character of the phosphite moiety increases reaction rates; 3) the flexibility and larger bite angle created by the biaryl phosphite moiety increases versatility; and 4) their modular nature enables the substituents/configurations in the oxazoline/oxazine moiety, alkyl backbone chain and in the biaryl phosphite moiety to be easily and systematically varied. By carefully selecting the ligand components, therefore, high regio- and enantioselectivities (*ee* up to 99%) and good activities have been achieved in a broad range of mono- and disubstituted linear hindered and unhindered substrates and cyclic substrates. These results are among the best reported. In general, activities and enantioselectivies are mainly affected by the substituents at the oxazoline and at the alkyl backbone chain, the presence of a second stereogenic center in the oxazoline ring, the size of the heterocycle, the substituents/configuration in the biaryl phosphite moiety and the cooperative effect between stereocenters. However, the effect of these parameters depends on each substrate class. It should be noted the excellent regio- (up to >95%) and enantioselectivities (up to 95% *ee*) combined with good activities obtained for monosubstitued substrates **S6** and **S7**. In addition, for substrates **S1**, **S2**, **S6** and **S7**, both enantiomers of substitution products can be obtained with high enantioselectivities by simply changing either the absolute configuration of the alkyl backbone chain or the absolute configuration of the biaryl phosphite moiety.

Study of the Pd–1,3-diphenyl-, 1,3-dimethyl- and 1,3-cyclohexenylallyl intermediates by NMR spectroscopy makes it possible to understand the catalytic behaviour observed. It also indicates that the nucleophilic attack takes place pre-

dominantly at the allylic terminal carbon atom located *trans* to the phosphite moiety. The study of the Pd–1,3-diphenylallyl and 1,3-cyclohexenylallyl intermediates also indicates that for enantioselectivities to be high, the substituents at the alkyl backbone chain and the electronic/steric properties at the oxazoline substituents need to be correctly combined in order to form predominantly the isomer that reacts faster with the nucleophile and also to avoid the formation of species with ligands coordinated in monodentated fashion. However, for the Pd–1,3-methylallyl intermediates the difference in enantioselectivity observed cannot be explained by the reactivity of the nucleophile *versus* the different π-allyl intermediates. We found a good explanation in the enhancement of the steric interaction upon attack of the nucleophile.

Experimental Section

General considerations: All reactions were carried out using standard Schlenk techniques under an atmosphere of argon. Solvents were purified and dried by standard procedures. Phosphorochloridites are easily prepared in one step from the corresponding biaryls.[23] Compounds **7,**[10] **8,**[24] **9,**[25] **11,**[26] **12,**[25] **14–15,**[24] **16,**[25] **19,**[25] **20,**[27] **21–22,**[24] **23,**[25] **25,**[26] **26,**[25] **27,**[24] **30–31,**[24] **34,**[28] **36–40**[9b] have been previously prepared. Racemic substrates **S1–S7** were prepared as previously reported.[29–32] $[Pd(\eta^3\text{-}1,3\text{-}Ph_2\text{-}C_3H_3)(\mu\text{-}Cl)]_2$,[33] $[Pd(\eta^3\text{-}1,3\text{-}Me_2\text{-}C_3H_3)(\mu\text{-}Cl)]_2$[34] and $[Pd(\eta^3\text{-}cyclohexenyl)(\mu\text{-}Cl)]_2$[35] were prepared as previously described. ^1H, $^{13}C\{^1H\}$, and $^{31}P\{^1H\}$ NMR spectra were recorded using a 400 MHz spectrometer. Chemical shifts are relative to that of $SiMe_4$ (^1H and ^{13}C) as internal standard or H_3PO_4 (^{31}P) as external standard. ^1H, ^{13}C and ^{31}P assignments were done based on ^1H–^1H gCOSY, ^1H–^{13}C gHSQC and ^1H–^{31}P gHMBC experiments.

General procedure for the preparation of amides: To a solution of the corresponding acyl chloride (25 mmol) in CH_2Cl_2 (200 mL) was added in one portion the corresponding hydroxyl amino acid (25 mmol). A solution of triethylamine (19.4 mL, 50 mmol) in CH_2Cl_2 (50 mL) was slowly added at 0 °C. The resulting mixture was stirred at room temperature for 3 h. The solvent was removed in vacuo and the residue purified by chromatography to afford the corresponding amides **8–14, 33, 36, 39, 42** (see Supporting Information).

General procedure for the preparation of oxazoline/oxazine esters: To a solution of the corresponding amide (10 mmol) in CH_2Cl_2 (40 mL) was added dropwise diethylaminosulfur trifluoride (1.45 mL, 11 mmol) at −78 °C. This solution was then stirred at this temperature for 1 h. Anhydrous K_2CO_3 (2.07 g, 15 mmol) was added in one portion and the reaction mixture allowed to warm to room temperature. After 2 h, saturated $NaHCO_3$ (aq) (50 mL) was added and the organic layer separated, dried over $MgSO_4$, filtered and the solvent removed in vacuum. The residue was purified by chromatography to give the desired oxazoline esters **15–21, 34, 37, 40** and oxazine ester **43** (see Supporting Information).

General procedure for the reduction of the oxazoline esters with $LiAlH_4$: To a solution of the corresponding oxazoline ester (10 mmol) in diethyl ether (50 mL) was added in five portions over ten minutes $LiAlH_4$ (0.42 g, 11 mmol) at 0 °C. After stirring for 15 min, ethyl acetate (25 mL) was added then water (40 mL). The organic layer was separated, dried over $MgSO_4$, filtered and the solvent removed in vacuo. The residue was purified by chromatography to give the desired oxazoline alcohols **22–26** (see Supporting Information).

General procedure for the reduction of the oxazoline esters with Grignard reagents: To a solution of the corresponding oxazoline ester (10 mmol) in THF/diethyl ether 1:1 (50 mL) was added dropwise a solution of the Grignard reagent in THF (11 mmol) at 0 °C. The mixture was then stirred for 3 h, allowed to warm to room temperature and stirred overnight. The reaction was quenched with saturated NH_4Cl aq (50 mL) and followed by the addition of additional diethyl ether (40 mL) and water (40 mL). The organic layer was separated, washed with water, dried over $MgSO_4$, filtered and the solvent removed in vacuo. The residue was purified by chromatography to give the desired tertiary oxazoline alcohols **27–32**, **35**, **38**, **41**, **44** (see Supporting Information).

General procedure for the preparation of the phosphite–oxazoline and phosphite–oxazine ligands L1–L15 a–h: The corresponding phosphorochloridite (3.0 mmol) produced in situ was dissolved in toluene (12.5 mL) and pyridine (1.14 mL, 14 mmol) was added. The corresponding hydroxyl-oxazoline/oxazine compound (2.8 mmol) was azeotropically dried with toluene (3×2 mL) and then dissolved in toluene (12.5 mL) to which pyridine (1.14 mL, 14 mmol) was added. The oxazoline/oxazine solution was transferred slowly at 0 °C to the solution of phosphorochloridite. The reaction mixture was stirred overnight at 80 °C, and the pyridine salts were removed by filtration. Evaporation of the solvent gave a white foam, which was purified by flash chromatography in alumina to produce the corresponding ligand as a white solid (for characterization see Supporting Information).

General procedure for the preparation of $[Pd(\eta^3\text{-allyl})(L)]BF_4$ complexes 55–62: The corresponding ligand (0.05 mmol) and the complex $[Pd(\mu\text{-}Cl)(\eta^3\text{-}1,3\text{-allyl})]_2$ (0.025 mmol) were dissolved in CD_2Cl_2 (1.5 mL) at room temperature under argon. $AgBF_4$ (9.8 mg, 0.5 mmol) was added after 30 minutes and the mixture was stirred for 30 minutes. The mixture was then filtered over Celite under argon and the resulting solutions were analyzed by NMR. After the NMR analysis, the complexes were precipitated adding hexane as pale yellow solids (for characterization see Supporting Information).

Study of the reactivity of the $[Pd(\eta^3\text{-allyl})(L))]BF_4$ with sodium malonate by in situ NMR:[36] A solution of in situ prepared $[Pd(\eta^3\text{-allyl})(\mathbf{L})]BF_4$ (L = phosphite-oxazoline, 0.05 mmol) in CD_2Cl_2 (1 mL) was cooled in the NMR at −80 °C. At this temperature, a solution of cooled sodium malonate (0.1 mmol) was added. The reaction was then followed by ^{31}P NMR. The relative reaction rates were calculated using a capillary containing a solution of triphenylphosphine in CD_2Cl_2 as external standard.

Typical procedure of allylic alkylation of *rac*-1,3-diphenyl-3-acetoxyprop-1-ene (S1): A degassed solution of $[PdCl(\eta^3\text{-}C_3H_5)]_2$ (0.9 mg, 0.0025 mmol) and the corresponding phosphite–oxazoline/oxazine (0.0055 mmol) in dichloromethane (0.5 mL) was stirred for 30 min. Subsequently, a solution of **S1** (126 mg, 0.5 mmol) in dichloromethane (1.5 mL), dimethyl malonate (171 μL, 1.5 mmol), *N*,*O*-bis(trimethylsilyl)acetamide (370 μL, 1.5 mmol) and a pinch of the corresponding base were added. The reaction mixture was stirred at room temperature. After the desired reaction time the reaction mixture was diluted with Et_2O (5 mL) and saturated NH_4Cl (aq) (25 mL) was added. The mixture was extracted with Et_2O (3×10 mL) and the extract dried over $MgSO_4$. Solvent was removed and conversion was measured by ^1H NMR. To determine the *ee* by HPLC (Chiralcel OD, 0.5% 2-propanol/hexane, flow 0.5 mL min^{-1}), a sample was filtered over basic alumina using dichloromethane as the eluent.[37]

Typical procedure of allylic alkylation of *rac*-(*E*)-ethyl 2,5-dimethyl-3-hex-4-enylcarbonate (S2): A degassed solution of $[PdCl(\eta^3\text{-}C_3H_5)]_2$ (1.8 mg, 0.005 mmol) and the phosphite–oxazoline/oxazine (0.011 mmol) in dichloromethane (0.5 mL) was stirred for 30 min. Subsequently, a solution of **S2** (107.2 mg, 0.5 mmol) in dichloromethane (1.5 mL), dimethyl malonate (171 μL, 1.5 mmol), *N*,*O*-bis(trimethylsilyl)-acetamide (370 μL, 1.5 mmol) and a pinch of KOAc were added. The reaction mixture was stirred at room temperature. After the desired reaction time, the reaction mixture was diluted with Et_2O (5 mL) and a saturated NH_4Cl (aq) (25 mL) was added. The mixture was extracted with Et_2O (3×10 mL) and the extract dried over $MgSO_4$. Conversion and enantiomeric excess was determined by ^1H NMR using $[Eu(hfc)_3]$ as resolving agent.[38]

Typical procedure of allylic alkylation of *rac*-1,3-dimethyl-3-acetoxyprop-1-ene (S3): A degassed solution of $[PdCl(\eta^3\text{-}C_3H_5)]_2$ (0.9 mg, 0.0025 mmol) and the corresponding phosphite–oxazoline/oxazine (0.0055 mmol) in dichloromethane (0.5 mL) was stirred for 30 min. Subsequently, a solution of **S3** (64 mg, 0.5 mmol) in dichloromethane (1.5 mL), dimethyl malonate (171 μL, 1.5 mmol), *N*,*O*-bis(trimethylsilyl)-

acetamide (370 μL, 1.5 mmol) and a pinch of KOAc were added. The reaction mixture was stirred at the desired temperature. After the desired reaction time, the resulting mixture was diluted with Et_2O (5 mL) and saturated NH_4Cl (aq) (25 mL) was added. The mixture was extracted with Et_2O (3×10 mL) and the extract dried over $MgSO_4$. Conversion and enantiomeric excess was determined by GC.[39]

Typical procedure of allylic alkylation of *rac*-3-acetoxycyclohexene (S4) and *rac*-3-acetoxycycloheptene (S5): A degassed solution of $[PdCl(\eta^3\text{-}C_3H_5)]_2$ (0.9 mg, 0.0025 mmol) and the corresponding phosphite–oxazoline/oxazine (0.0055 mmol) in dichloromethane (0.5 mL) was stirred. After 30 minutes the solution was kept to the desired temperature and subsequently, a solution of racemic substrate (0.5 mmol) in dichloromethane (1.5 mL) at the desired temperature, dimethyl malonate (171 μL, 1.5 mmol), *N*,*O*-bis(trimethylsilyl)acetamide (370 μL, 1.5 mmol) and a pinch of KOAc were added. The reaction mixture was stirred at the desired temperature. After the desired reaction time, the reaction mixture was diluted with Et_2O (5 mL) and saturated NH_4Cl (aq) (25 mL) was added. The mixture was extracted with Et_2O (3×10 mL) and the extract dried over $MgSO_4$. Conversion and enantiomeric excess was determined by GC.[40]

Typical procedure of allylic alkylation of 1-(1-naphthyl)allyl acetate (S6) and 1-(1-naphthyl)-3-acetoxyprop-1-ene (S7): A degassed solution of $[PdCl(\eta^3\text{-}C_3H_5)]_2$ (1.8 mg, 0.005 mmol) and the corresponding phosphite–oxazoline/oxazine (0.011 mmol) in dichloromethane (0.5 mL) was stirred for 30 min at room temperature. Subsequently, a solution of substrate (0.5 mmol) in dichloromethane (1.5 mL), dimethyl malonate (171 μL, 1.5 mmol), *N*,*O*-bis(trimethylsilyl)acetamide (370 μL, 1.5 mmol) and a pinch of KOAc were added. After 2 h at room temperature, the reaction mixture was diluted with Et_2O (5 mL) and saturated NH_4Cl (aq) (25 mL) was added. The mixture was extracted with Et_2O (3×10 mL) and the extract dried over $MgSO_4$. Solvent was removed and conversion and regioselectivity were measured by ^1H NMR. To determine the ee by HPLC (Chiralcel OJ, 13% 2-propanol/hexane, flow 0.7 mL min^{-1}), a sample was filtered over basic alumina using dichloromethane as the eluent.[40]

Typical procedure of allylic amination of *rac*-1,3-diphenyl-3-acetoxyprop-1-ene (S1): A degassed solution of $[PdCl(\eta^3\text{-}C_3H_5)]_2$ (0.9 mg, 0.0025 mmol) and the corresponding phosphite–oxazoline/oxazine (0.0055 mmol) in dichloromethane (0.5 mL) was stirred for 30 min. Subsequently, a solution of **S1** (126 mg, 0.5 mmol) in dichloromethane (1.5 mL) and benzylamine (131 μL, 1.5 mmol) were added. The reaction mixture was stirred at room temperature. After the desired reaction time, the reaction mixture was diluted with Et_2O (5 mL) and saturated NH_4Cl (aq) (25 mL) was added. The mixture was extracted with Et_2O (3×10 mL) and the extract dried over $MgSO_4$. Solvent was removed and conversion was measured by ^1H NMR. To determine the *ee* by HPLC (Chiralcel OJ, 13% 2-propanol/hexane, flow 0.5 mL min^{-1}), a sample was filtered over silica using 10% Et_2O/hexane mixture as the eluent.[38]

Typical procedure of allylic amination of *rac*-(*E*)-ethyl 2,5-dimethyl-3-hex-4-enylcarbonate (S2): A degassed solution of $[PdCl(\eta^3\text{-}C_3H_5)]_2$ (1.8 mg, 0.005 mmol) and the corresponding phosphite–oxazoline/oxazine (0.011 mmol) in dichloromethane (0.5 mL) was stirred for 30 min. Subsequently, a solution of **S2** (107.2 mg, 0.5 mmol) in dichloromethane (1.5 mL) and benzylamine (131 μL, 1.5 mmol) were added. The reaction mixture was stirred at room temperature. After the desired reaction time, the reaction mixture was diluted with Et_2O (5 mL) and saturated NH_4Cl (aq) (25 mL) was added. The mixture was extracted with Et_2O (3×10 mL) and the extract dried over $MgSO_4$. Conversion and enantiomeric excess was determined by GC.[39]

Typical procedure of allylic amination of *rac*-1,3-dimethyl-3-acetoxyprop-1-ene (S3): A degassed solution of $[PdCl(\eta^3\text{-}C_3H_5)]_2$ (0.9 mg, 0.0025 mmol) and the corresponding phosphite–oxazoline/oxazine (0.0055 mmol) in dichloromethane (0.5 mL) was stirred for 30 min. Subsequently, a solution of **S3** (64 mg, 0.5 mmol) in dichloromethane (1.5 mL) and benzylamine (131 μL, 1.5 mmol) were added. The reaction mixture was stirred at room temperature. After the desired reaction time, the reaction mixture was diluted with Et_2O (5 mL) and saturated NH_4Cl (aq) (25 mL) was added. The mixture was extracted with Et_2O (3×10 mL) and the extract dried over $MgSO_4$. Conversion and enantiomeric excess was determined by GC.[39]

Acknowledgements

We are indebted to Professor P. W. N. M. van Leeuwen, University of Amsterdam, and Dr. Carles Bó, Institut Català d'Investigació Química (ICIQ), for their comments and suggestions on the mechanistic aspects and theoretical calculations, respectively. We thank the Spanish Government (Consolider Ingenio CSD2006-0003, CTQ2004-04412/BQU and the Ramon y Cajal fellowship to O.P.) and the Catalan Government (2005SGR007777 and Distinction to M.D.) for financial support.

[1] For recent reviews, see: a) J. Tsuji in *Palladium Reagents and Catalysis, Innovations in Organic Synthesis*, Wiley, New York, **1995**; b) B. M. Trost, D. L. van Vranken, *Chem. Rev.* **1996**, *96*, 395; c) M. Johannsen, K. A. Jorgensen, *Chem. Rev.* **1998**, *98*, 1689; d) A. Pfaltz, M. Lautens in *Comprehensive Asymmetric Catalysis, Vol. 2* (Eds.: E. N. Jacobsen, A. Pfaltz, H. Yamamoto), Springer, Berlin, **1999**, Chapter 24; e) B. M. Trost, M. L. Crawley, *Chem. Rev.* **2003**, *103*, 2921.

[2] See for instante: a) A. M. Masdeu-Bultó, M. Diéguez, E. Martin, M. Gómez, *Coord. Chem. Rev.* **2003**, *242*, 159; b) E. Martín, M. Diéguez, *C. R. Chemie* **2007**, *10*, 188.

[3] See e.g.: a) E. Raluy, C. Claver, O. Pàmies, M. Diéguez, *Org. Lett.* **2007**, *9*, 49; b) M. Diéguez, O. Pàmies, C. Claver, *Adv. Synth. Catal.* **2007**, *349*, 836; c) O. Pàmies, M. Diéguez, *Chem. Eur. J.* **2008**, *14*, 944.

[4] a) G. Helmchen, A. Pfaltz, *Acc. Chem. Res.* **2000**, *33*, 336; b) G. J. Dawson, C. G. Frost, J. M. J. Williams, *Tetrahedron Lett.* **1993**, *34*, 3149; c) B. Wiene, G. Helmchen, *Tetrahedron Lett.* **1998**, *39*, 5727; d) P. von Matt, A. Pfaltz, *Angew. Chem.* **1993**, *105*, 614; *Angew. Chem. Int. Ed. Engl.* **1993**, *32*, 566; e) P. Sennhenn, B. Gabler, G. Helmchen, *Tetrahedron Lett.* **1994**, *35*, 8595.

[5] O. Pàmies, M. Diéguez, C. Claver, *J. Am. Chem. Soc.* **2005**, *127*, 3646.

[6] a) G. P. F. van Strijdonck, M. D. K. Boele, P. C. J. Kamer, J. G. de Vries, P. W. N. M. van Leeuwen, *Eur. J. Inorg. Chem.* **1999**, 1073; b) M. Diéguez, O. Pàmies, C. Claver, *Adv. Synth. Catal.* **2005**, *347*, 1257; c) M. Diéguez, O. Pàmies, C. Claver, *J. Org. Chem.* **2005**, *70*, 3363.

[7] The flexibility that offers the biphenyl moiety can be used to fine tune the chiral pocket formed upon complexation. See for example: a) ref. [5]; b) Y. Mata, M. Diéguez, O. Pàmies, C. Claver, *Adv. Synth. Catal.* **2005**, *347*, 1943.

[8] R. Prétôt, A. Pfaltz, *Angew. Chem.* **1998**, *110*, 337; *Angew. Chem. Int. Ed.* **1998**, *37*, 323.

[9] a) K. N. Gavrilov, V. N. Tsarev, S. V. Zheglov, S. E. Lyubimov, A. A. Shyryaev, P. V. Petrovskii, V. A. Davankov, *Mendeleev Commun.* **2004**, 260; b) R. Hilgraf; A. Pfaltz, *Adv. Synth. Catal.* **2005**, *347*, 61; A. Pfaltz, *Adv. Synth. Catal.* **2005**, *347*, 61.

[10] T. Kline, N. H. Andersen, E. A. Harwood, J. Bowman, A. Malanda, S. Endsley, A. L. Erwin, M. Doyle, S. Fong, A. L. Harris, B. Mendelson, K. Mdluli, C. R. H. Raetz, C. K. Stover, P. R. Witte, A. Yabannavar, S. Zhu, *J. Med. Chem.* **2002**, *45*, 3112.

[11] O. Pàmies, M. Diéguez, G. Net, A. Ruiz, C. Claver, *Organometallics* **2000**, *19*, 1488.

[12] Atropoisomerization of the biaryl moiety is usually stopped upon coordination to the metal center. See for example: a) G. J. H. Buisman, L. A. van der Veen, A. Klootwijk, W. G. J. de Lange, P. C. J. Kamer, P. W. M. N. van Leeuwen, D. Vogt, *Organometallics* **1997**, *16*, 2929; b) M. Diéguez, O. Pàmies, A. Ruiz, C. Claver, S. Castillón, *Chem. Eur. J.* **2001**, *7*, 3086; c) O. Pàmies, M. Diéguez, G. Net, A. Ruiz, C. Claver, *J. Org. Chem.* **2001**, *66*, 8364; d) M. Diéguez, O. Pàmies, A. Ruiz, C. Claver, *New J. Chem.* **2002**, *26*, 827.

[13] For some successful applications, see: a) P. Dierkes, S. Randechul, L. Barloy, A. De Cian, J. Fischer, P. C. J. Kamer, P. W. N. M. van Leeuwen, J. A. Osborn, *Angew. Chem.* **1998**, *110*, 3299; *Angew. Chem. Int. Ed.* **1998**, *37*, 3116; b) B. M. Trost, A. C. Krueger, R. C. Bunt, J. Zambrano, *J. Am. Chem. Soc.* **1996**, *118*, 6520; c) refs. [4c], [5] and [7b].

[14] For more successful applications, see: a) B. M. Trost, R. C. Bunt, *J. Am. Chem. Soc.* **1994**, *116*, 4089; b) G. Helmchen, S. Kudis, P. Sennhenn, H. Steinhagen, *Pure Appl. Chem.* **1997**, *69*, 513.

[15] In contrast to the Pd-catalytic systems, the Ir, Ru and Mo catalysts provide very high selectivity for the attack to the non-terminal carbon to give the chiral product. See e.g. a) C. Bruneau, J. L. Renaud, B. Demersemen, *Chem. Eur. J.* **2006**, *12*, 5178; b) A. V. Malkov, L. Gouriou, G. C. Lloyd-Jones, I. Starý, V. Langer, P. Spoor, V. Vinader, P. Koèovský, *Chem. Eur. J.* **2006**, *12*, 6910; c) B. M. Trost, S. Hildbrand, K. Dogra, *J. Am. Chem. Soc.* **1999**, *121*, 10416; d) A. Alexakis, D. Polet, *Org. Lett.* **2004**, *6*, 3529.

[16] For recent successful applications of Pd-catalysts, see: a) S.-L. You, X.-Z. Zhu, Y.-M. Luo, X.-L. Hou, L.-X. Dai, *J. Am. Chem. Soc.* **2001**, *123*, 7471; b) R. Hilgraf, A. Pfaltz, *Synlett* **1999**, 1814.

[17] a) S. Deerenberg, H. S. Schrekker, G. P. F. van Strijdonck, P. C. J. Kamer, P. W. N. M. van Leeuwen, J. Fraanje, K. Goubitz, *J. Org. Chem.* **2000**, *65*, 4810; b) E. Fernández, M. Gómez, S. Jansat, G. Muller, E. Martín, L. Flores Santos, P. X. García, A. Acosta, A. Aghmiz, M. Jiménez-Pedrós, A. M. Masdeu-Bultó, M. Diéguez, C. Claver, M. A. Maestro, *Organometallics* **2005**, *24*, 3946.

[18] The equilibrium between both diastereoisomers takes place via the so-called apparent π-allyl rotation. Three main mechanism for this has been proposed. One of them involves π–σ–π isomerization followed by rotation around the Pd–C bond in the η^1 intermediate. The other one has been shown to occur via dissociation of one of the coordinated atoms of the bidentate ligand, which allows the ligand to rotate, see: a) A. Gogoll, J. Örnebro, H. Grennberg, J. E. Bäckvall, *J. Am. Chem. Soc.* **1994**, *116*, 3631; b) P. S. Pregosin, R. Salzmann, *Coord. Chem. Rev.* **1996**, *155*, 35; c) S. Hansson, P. O. Norrby, M. P. T. Sjören, B. Åkermark, M. E. Cucciolito, F. Giordano, A. Vitagliano, *Organometallics* **1993**, *12*, 4940.

[19] S. Schaffner, J. F. K. Müller, M. Neuburger, M. Zehner, *Helv. Chim. Acta* **1998**, *81*, 1223.

[20] These results also indicate that *syn*/*syn* **A** to *syn*/*syn* **B** interconversion should be faster than the nucleophilic attack.

[21] The study of the models has been performed using molecular mechanics calculations using the universal force field (UFF).

[22] A. M. Porte, J. Reibenspies, K. Burgess, *J. Am. Chem. Soc.* **1998**, *120*, 9180.

[23] G. J. H. Buisman, P. C. J. Kamer, P. W. N. M. van Leeuwen, *Tetrahedron: Asymmetry* **1993**, *4*, 1625.

[24] G. Jones, C. J. Richards, *Tetrahedron: Asymmetry* **2004**, *15*, 653.

[25] S. Nanchen, A. Pfaltz, *Chem. Eur. J.* **2006**, *12*, 4550.

[26] D. Franco, M. Gómez, F. Jiménez, G. Muller, M. Rocamora, M. A. Maestro, J. Mahía, *Organometallics* **2004**, *23*, 3197.

[27] M. C. Pirrung, L. N. Tumey, *J. Comb. Chem.* **2000**, *2*, 675.

[28] a) A. L. Braga, F. Vargas, J. A. Sehnem, R. C. Braga, *J. Org. Chem.* **2005**, *70*, 9021; b) J. Chen, Y. Li, X.-P. Cao, *Tetrahedron: Asymmetry* **2006**, *17*, 933.

[29] P. R. Auburn, P. B. Mackenzie, B. Bosnich, *J. Am. Chem. Soc.* **1985**, *107*, 2033.

[30] C. Jia, P. Müller, H. Mimoun, *J. Mol. Catal. A* **1995**, *101*, 127.

[31] J. Lehman, G. C. Lloyd-Jones, *Tetrahedron* **1995**, *51*, 8863.

[32] T. Hayashi, A. Yamamoto, Y. Ito, E. Nishioka, H. Miura, K. Yanagi, *J. Am. Chem. Soc.* **1989**, *111*, 6301.

[33] P. von Matt, G. C. Lloyd-Jones, A. B. E. Minidis, A. Pfaltz, L. Macko, M. Neuburger, M. Zehnder, H. Ruegger, P. S. Pregosin, *Helv. Chim. Acta* **1995**, *78*, 265.

[34] M. Kollmar, B. Goldfuss, M. Reggelin, F. Rominger, G. Helmchen, *Chem. Eur. J.* **2001**, *7*, 4913.

[35] B. M. Trost, P. E. Strege, L. Weber, *J. Am. Chem. Soc.* **1978**, *100*, 3407.

[36] R. J. van Haaren, P. H. Keeven, L. A. van der Veen, K. Goubitz, G. P. F. van Strijdonck, H. Oevering, J. N. H. Reek, P. C. J. Kamer, P. W. N. M. van Leeuwen, *Inorg. Chim. Acta* **2002**, *327*, 108.

[37] O. Pàmies, G. P. F. van Strijdonck, M. Diéguez, S. Deerenberg, G. Net, A. Ruiz, C. Claver, P. C. J. Kamer, P. W. N. M. van Leeuwen, *J. Org. Chem.* **2001**, *66*, 8867.

[38] D. A. Evans, K. R. Campos, J. S. Tedrow, F. E. Michael, M. R. Gagné, *J. Am. Chem. Soc.* **2000**, *122*, 7905.

[39] M. A. Pericàs, C. Puigjaner, A. Riera, A. Vidal-Ferran, M. Gómez, F. Jiménez, G. Muller, M. Rocamora, *Chem. Eur. J.* **2002**, *8*, 4164.

[40] J. P. Janssen, G. Helmchen, *Tetrahedron Lett.* **1997**, *38*, 8025.

Received: October 15, 2007
Published online: February 27, 2008

